

# **SIMULATING THE VARIABLE-SOURCE-AREA CONCEPT OF STREAMFLOW GENERATION WITH THE WATERSHED MODEL TOPMODEL**

**By David M. Wolock**

---

**U.S. GEOLOGICAL SURVEY**

**Water-Resources Investigations Report 93-4124**



**Lawrence, Kansas**

**1993**

**U.S. DEPARTMENT OF THE INTERIOR**

**BRUCE BABBITT, Secretary**

**U.S. GEOLOGICAL SURVEY**

**Robert M. Hirsch, Acting Director**

---

**For additional information write to:**

District Chief  
U.S. Geological Survey  
Water Resources Division  
4821 Quail Crest Place  
Lawrence, Kansas 66049-3839

**Copies of this report can be  
purchased from:**

U.S. Geological Survey  
Books and Open-File Reports  
Denver Federal Center  
Box 25425  
Denver, Colorado 80225

# CONTENTS

	Page
Abstract .....	1
Introduction.....	1
Concepts of streamflow generation .....	1
Movement of water through a watershed in TOPMODEL .....	2
Differences among versions of TOPMODEL .....	6
Simulating streamflow generation with TOPMODEL .....	7
TOPMODEL equations .....	7
Streamflow generation .....	7
Spatial aggregation .....	11
Snow accumulation and melt .....	13
Evapotranspiration .....	14
Impervious areas .....	14
Channel routing .....	14
Setting model parameters .....	14
Soil hydraulic parameters .....	14
Spatial distribution of $\ln(a / \tan B)$ .....	15
Frequency distribution of $\ln(a / \tan B)$ .....	21
Spatial and frequency distributions of $\ln[a / (T_0 \tan B)]$ .....	22
Channel-routing parameters .....	22
Calibration of model parameters .....	22
Using the TOPMODEL Fortran program .....	23
Potential future directions for TOPMODEL .....	29
References.....	30

# ILLUSTRATIONS

	Page
Figures 1-7.--Diagrams showing:	
1. Streamflow-generation mechanism during low-flow periods .....	2
2. Streamflow-generation mechanisms during high-flow periods .....	3
3. Water fluxes in TOPMODEL .....	4
4. Water fluxes when rainfall or snowmelt occurs on an unsaturated location in the watershed .....	5
5. Water fluxes when rainfall or snowmelt occurs on a saturated location in the watershed .....	6
6. Definition of terms in the continuity equation for location $x$ .....	9

## ILLUSTRATIONS

		Page
Figure	7. Relation between saturated hydraulic conductivity and soil depth .....	10
	8. Maps showing elevation and $\ln(a/\tan B)$ values for subbasin W-3 in Sleepers River watershed in Vermont.....	12
	9. Graph showing relative frequency distribution of $\ln(a/\tan B)$ values for Sleepers River watershed in Vermont.....	13
Figures 10-14.--Plan views showing:		
	10. Elevation grid file containing a depression highlighted in bold and same elevation file with depression removed after using the program concave .....	16
	11. Elevation grid file containing no depressions, grid of downslope directions produced by the program direct, and graphical representation of downslope directions .....	17
	12. Grid of downslope directions produced by the program direct and grid of number of upslope nodes.....	18
	13. Grid of elevations, grid of steepest downslope directions, and grid of $\tan B$ values .....	19
	14. Grid of number of upslope nodes, grid of $\tan B$ values, and grid of $\ln(a/\tan B)$ values .....	20
	15. Flow chart showing relations among major TOPMODEL components .....	24

## TABLES

		Page
Table	1. TOPMODEL input and output .....	7
	2. Programs used to compute the $\ln(a/\tan B)$ distribution and moments .....	15
	3. Contents of parameter file for TOPMODEL.....	25
	4. Corresponding parameter names in TOPMODEL Fortran code and in this report .....	26
	5. Corresponding variable names in TOPMODEL Fortran code and in this report .....	27
	6. Contents of input data file for TOPMODEL.....	28
	7. Contents of output file from TOPMODEL.....	29

## CONVERSION FACTORS<sup>1</sup> AND VERTICAL DATUM

<i><b>Multiply</b></i>	<i><b>By</b></i>	<i><b>To obtain</b></i>
centimeter	0.3937	inch
millimeter	0.03937	inch
meter	3.2808	foot
kilometer	0.6214	mile
square millimeter	0.00155	square inch
square kilometer	0.3861	square mile

Temperature can be converted to degrees Celsius (°C) or degrees Fahrenheit (°F) by the equations:

$$^{\circ}C = \frac{5}{9} (^{\circ}F - 32)$$

$$^{\circ}F = \frac{9}{5} (^{\circ}C) + 32.$$

Sea level: In this report, "sea level" refers to the National Geodetic Vertical Datum of 1929--a geodetic datum is derived from a general adjustment of the first-order level nets of the United States and Canada, formerly called Sea Level Datum of 1929.

---

<sup>1</sup> The algorithms in TOPMODEL use mostly metric units, but a few use English units. Compatibility between units in the algorithms is accomplished by unit conversions within the model computer code.



# **SIMULATING THE VARIABLE-SOURCE-AREA CONCEPT OF STREAMFLOW GENERATION WITH THE WATERSHED MODEL TOPMODEL**

**By David M. Wolock**

## **ABSTRACT**

TOPMODEL is a physically based watershed model that simulates the variable-source-area concept of streamflow generation. This report describes the theoretical background, model equations, methods to determine parameter values, Fortran computer code, and an example interactive simulation. Using TOPMODEL requires the specification of soils and topographic parameters, watershed latitude, and time series of precipitation and air temperature. Model predictions include, in addition to streamflow, estimates of overland and subsurface flow, and an estimate of the spatial pattern of the depth to the water table in the watershed.

## **INTRODUCTION**

TOPMODEL is a physically based watershed model that simulates the variable-source-area concept of streamflow generation. The model was first described in the literature in a paper by Beven and Kirkby (1979), but it is continuously evolving to reflect the current ideas of how precipitation moves over and through watersheds to become streamflow. TOPMODEL has been used to study a variety of research areas, including synthetic flood-frequency derivation (Beven, 1986a and b, 1987), model-parameter calibration (Hornberger and others, 1985; Wolock, 1988), carbon budget simulation (Band and others, 1991), spatial scale effects on hydrologic processes (Sivapalan and others, 1987, 1990; Beven and others, 1988; Wood and others, 1988, 1990; Famiglietti and Wood, 1991; Famiglietti, 1992), topographic effects on water quality (Wolock, 1988; Wolock and others, 1989, 1990), topographic effects on streamflow (Beven and Wood, 1983; Beven and others, 1984; Kirkby, 1986), effects of climate change on hydrologic processes (Wolock and Hornberger, 1991), and the geomorphic evolution of basins (Ijjasz-Vasquez and others, 1992).

The version of TOPMODEL described in this report is derived from the version described by Hornberger and others (1985), with extensive modification. The version described here was developed to study questions related to the estimation of model parameters from observable watershed characteristics and the calibration of parameters through optimization techniques (Wolock, 1988).

TOPMODEL is only one of a number of mathematical computer models that simulate the variable-source-area concept of streamflow generation. Other models include those described by Stephenson and Freeze (1974), Lee and Delleur (1976), Freeze (1980), Smith and Hebbert (1983), Bernier (1985), Bathurst (1986), Moore and others (1986), O'Loughlin (1986), Binley and others (1989), Ormsbee and Khan (1989), Prevost and others (1990), Moore and Grayson (1991), Grayson and others (1992), and Stagnitti and others (1992).

The purpose of this report is to describe the theoretical background of TOPMODEL, model equations, methods to determine parameter values, and the Fortran computer code. The report also provides an example interactive simulation.

## **Concepts of Streamflow Generation**

Concepts of streamflow-generation mechanisms describe how streamflow is produced. For example, it is a widely accepted concept that, during low-flow periods, streamflow is "generated" by the drainage of water from the saturated subsurface zone (fig. 1) into the stream channel (Dunne and Leopold, 1978).

A number of concepts have been developed to describe the generation of streamflow during high-flow periods; that is, during precipitation events. The main concepts discussed in the literature are schematically represented in figure 2. The first concept, called infiltration-excess overland flow (also called Horton overland flow), states that streamflow during



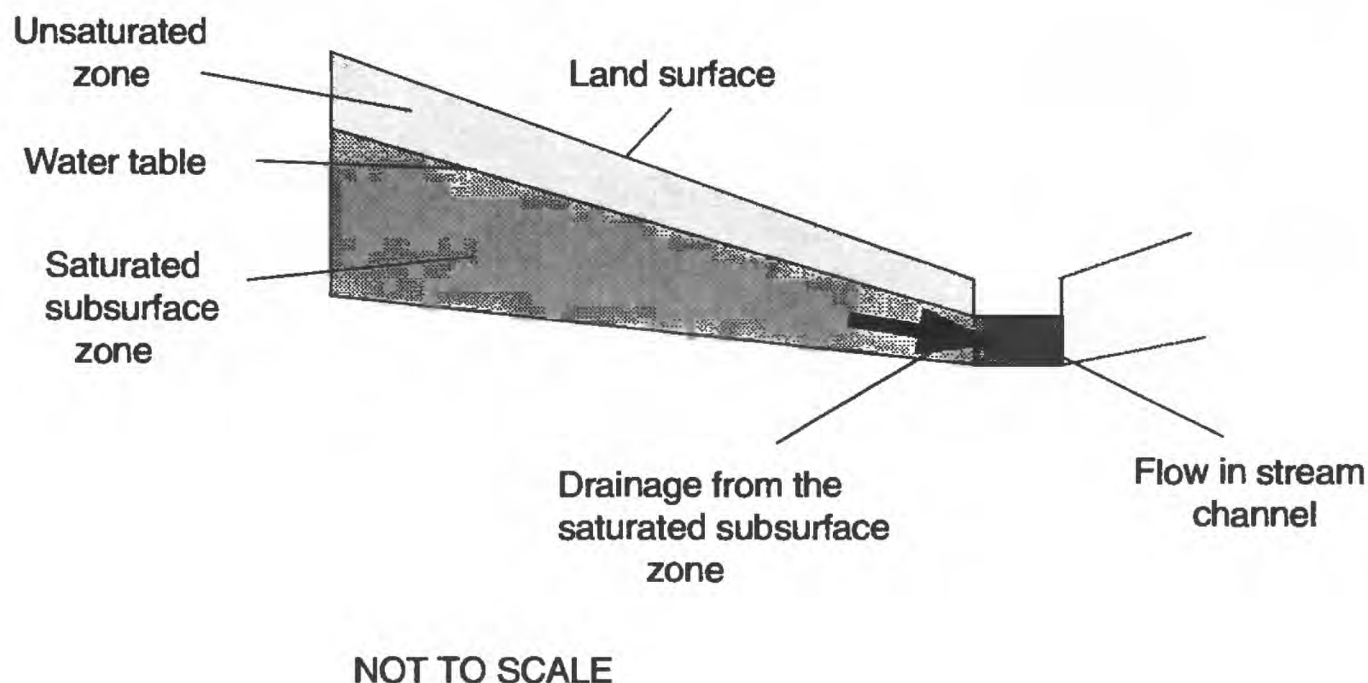


**Figure 1.** Streamflow-generation mechanism during low-flow periods.

precipitation events is generated by overland flow that is produced when precipitation rates exceed infiltration rates at the land-atmosphere interface (fig. 2). In the original concept of infiltration-excess overland flow, Horton (1933) assumed that streamflow during precipitation events was produced by overland flow generated throughout the entire area of a watershed. Later, Betson (1964) proposed that on some watersheds streamflow during precipitation events was generated from infiltration-excess overland flow produced on only a small part of the watershed area, an idea known as the "partial-area concept." Infiltration-excess overland flow occurs in areas where infiltration rates are less than precipitation rates; for example, in disturbed or poorly vegetated areas in subhumid and semiarid regions.

Another concept of streamflow generation during precipitation events is called the variable-source-area concept (fig. 2). The earliest published work that evolved into this concept is by Hursh (1936). In the variable-source-area concept, streamflow during precipitation events is generated on saturated surface areas called "source areas," which occur in places where the water table rises to the land surface (fig. 2). The rise in the water table occurs because of infiltration of precipitation into the soil and down to the saturated subsurface zone, and the subsequent downslope movement of water in the saturated subsurface zone. Saturated land-surface areas commonly develop near

existing stream channels and expand as more water enters the subsurface through infiltration and moves downslope as saturated subsurface flow. Variable-source-area flow occurs where infiltration rates are greater than precipitation rates; for example, in undisturbed vegetated areas in humid, temperate regions.

In the variable-source-area concept, saturated land-surface areas are sources of streamflow during precipitation events in several ways (fig. 2). Saturation overland flow (also called Dunne overland flow) is generated if the subsurface hydraulic characteristics are not transmissive and if slopes are gentle and convergent. Saturation overland flow can arise from direct precipitation on the saturated land-surface areas or from return flow of subsurface water to the surface in the saturated areas (fig. 2) (Dunne and Black, 1970). Subsurface stormflow (Hewlett and Hibbert, 1967) is generated if the near-surface soil zone is very transmissive (large saturated hydraulic conductivity) and if gravitational gradients (slopes) are steep (fig. 2).

### **Movement of Water Through a Watershed in TOPMODEL**

TOPMODEL simulates the movement of water through a watershed from the time that it enters the watershed as precipitation to the time that it exits the watershed as streamflow. The main paths that water follows during this



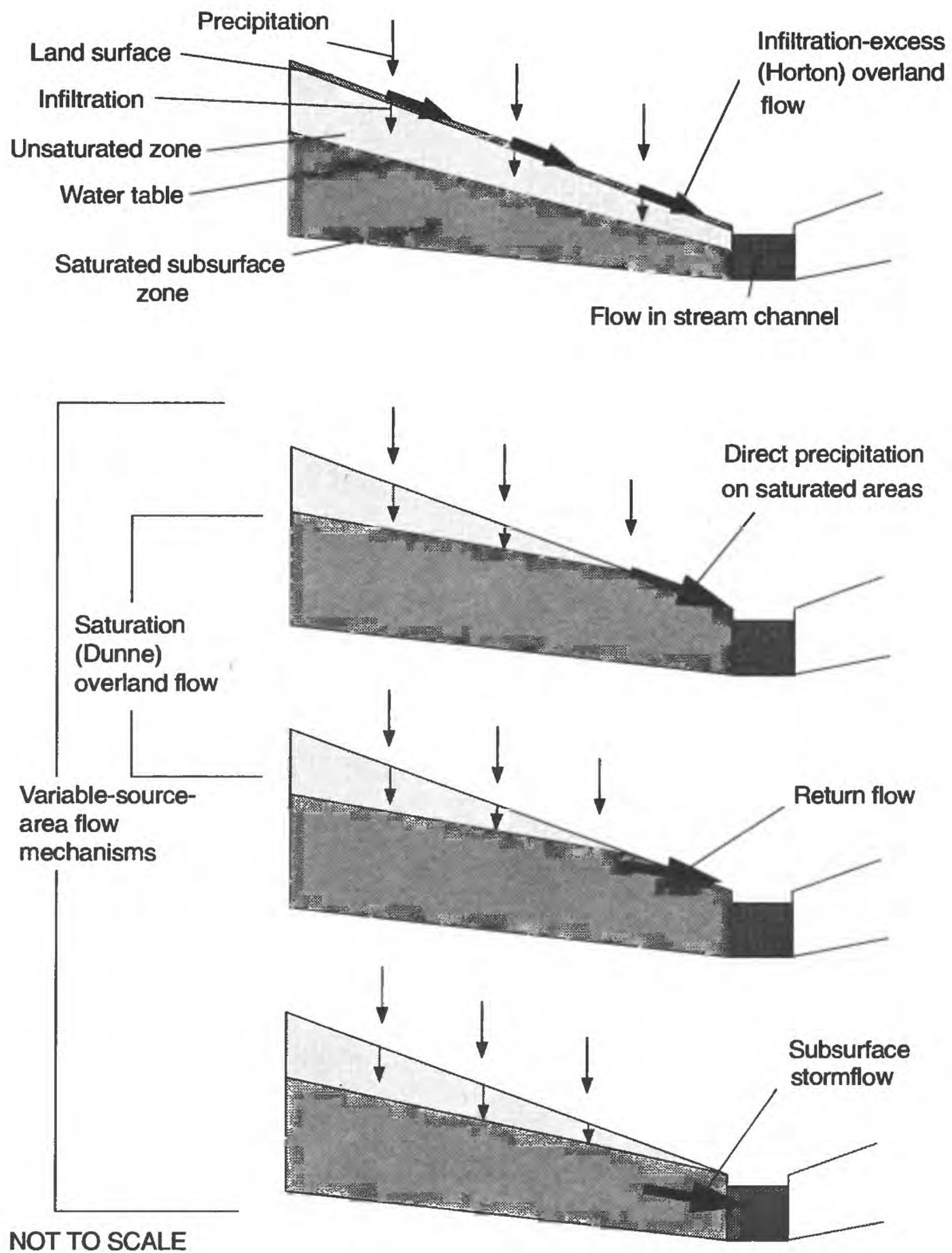


**Figure 2.** Streamflow-generation mechanisms during high-flow periods.

sequence are illustrated in figure 3. Precipitation enters the watershed as either rain or snow depending on the air temperature and TOPMODEL parameters. Air temperature and TOPMODEL parameters also determine the rate at which any accumulated snow melts.

The version of TOPMODEL described in this report simulates the variable-source-area concept of streamflow generation, not the Horton (1933) concept of infiltration-excess overland flow or the partial-area concept of Betson (1964). In the variable-source-area concept, rain (or snowmelt) infiltrates into the upper zone of the soil anywhere that the water table has not risen to the land surface (fig. 4). Water stored in the upper soil zone evaporates or transpires at a rate dependent on the potential evapotranspiration rate (computed from air temperature and latitude) and the amount of moisture available in the upper soil zone. Through macropores (large pores in the soil that

conduct water downward before the soil is completely saturated) some rain (or snowmelt) can bypass the unsaturated subsurface zone and move directly into the saturated subsurface zone (Beven and Germann, 1982).

The depth to the water table is decreased by water draining down from above or laterally from other parts of the watershed. If this contribution of water to the saturated subsurface zone at a particular location in the watershed is large enough, then the water table rises to the land surface, and the area becomes saturated. Saturation overland flow is produced by direct precipitation (rain or snowmelt) on saturated areas (fig. 5). The saturated land-surface area also can produce return flow if the water table rises above the land surface.

During all streamflow conditions, any water stored in the saturated subsurface zone is assumed to move downslope towards the stream

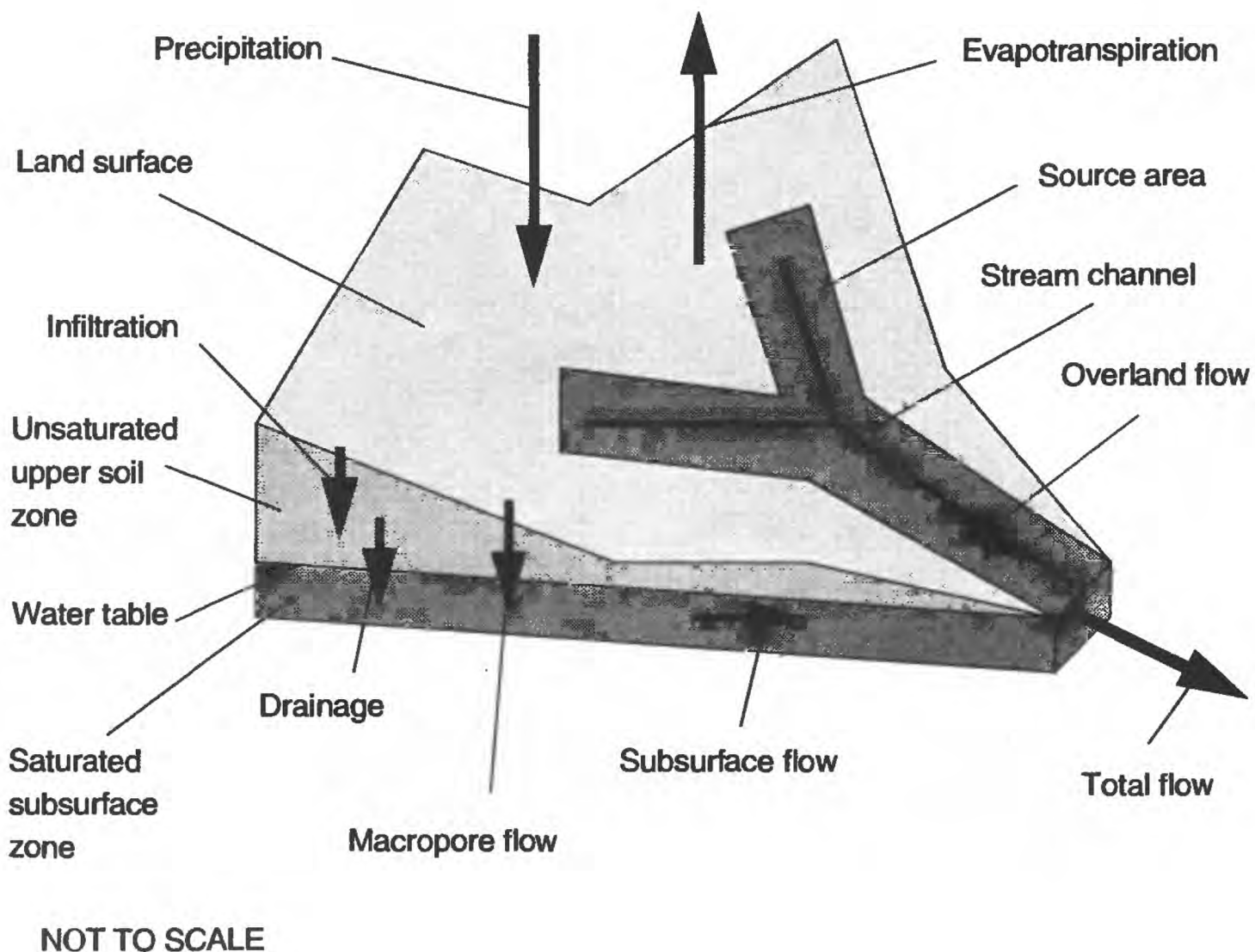


**Figure 3.** Water fluxes in TOPMODEL.

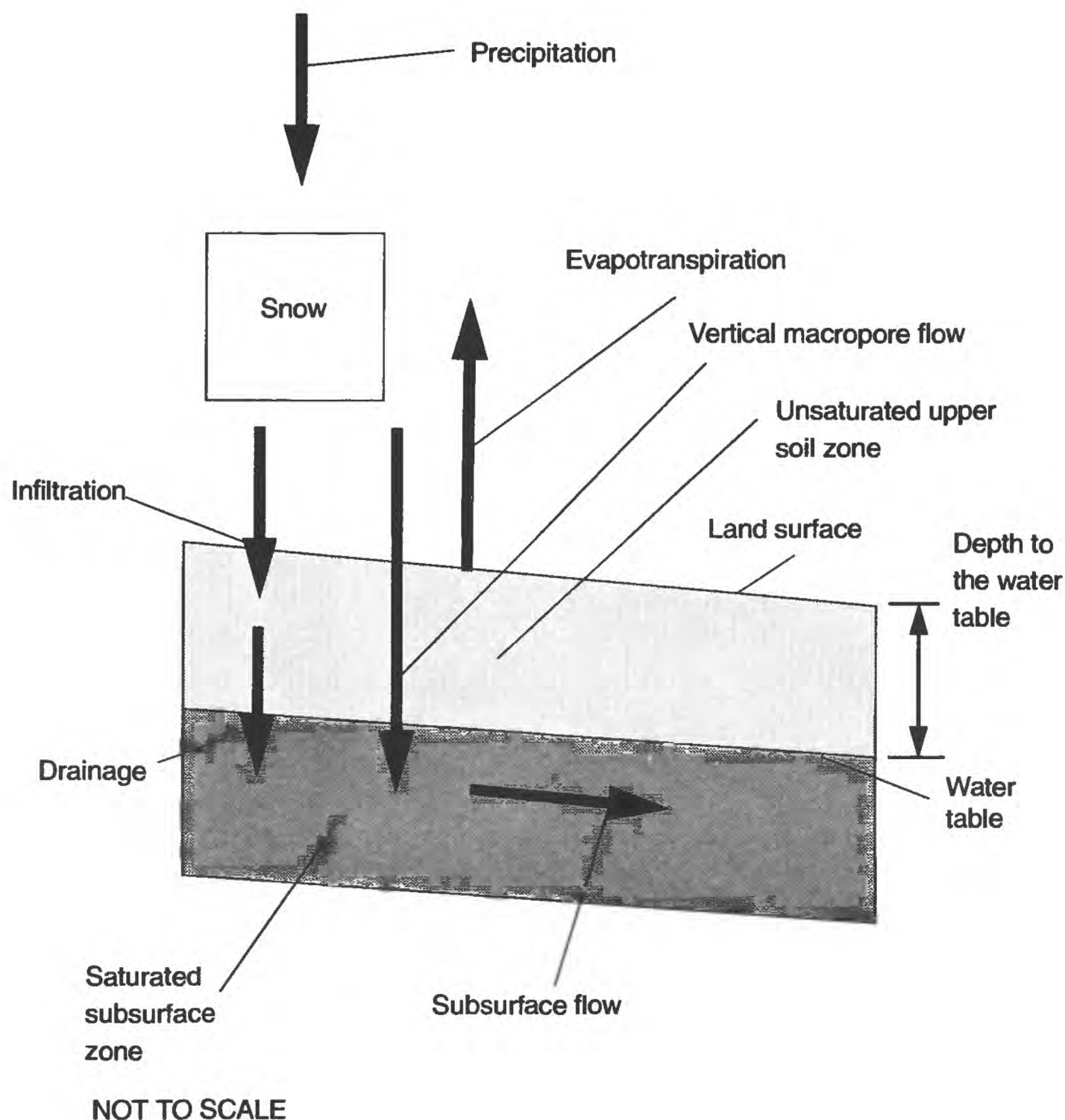


**Figure 4.** Water fluxes when rainfall or snowmelt occurs on an unsaturated location in the watershed.

channel. A portion of the water, depending on the volume stored and TOPMODEL parameters, drains into the stream. TOPMODEL assumes that the rate of subsurface flow into the stream increases exponentially as the water table moves closer to the land surface. This assumption is based on the idea that macropores can increase hydraulic transmissivity in the lateral direction and that macropores become increasingly abundant near the soil surface (Beven, 1984; Elsenbeer and others, 1992). Any drainage from the saturated subsurface zone into the stream increases the depth to the water table.

The location of source areas (the saturated land-surface areas) within the watershed are affected by basin topography and soil hydraulic characteristics. This is consistent with observed spatial distributions of soil moisture and potentiometric surfaces (for example, Kirkby and Chorley, 1967; Dunne and others, 1975; Anderson and Burt, 1978; Beven, 1978; Anderson and Kneale, 1980; O'Loughlin, 1981; Burt and Butcher, 1985). Source areas are found where subsurface water collects, locations where large upslope areas are drained, and where there is limited capacity for continued downslope movement. Topography, the three-



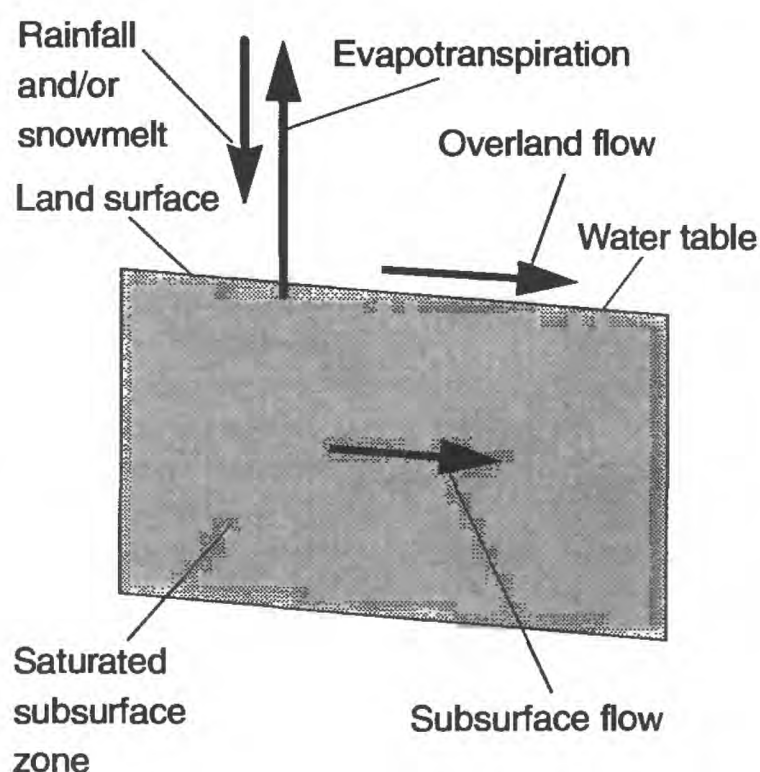


**Figure 5.** Water fluxes when rainfall or snowmelt occurs on a saturated location in the watershed.

dimensional configuration of gravitational effects on drainage, affects the location of source areas. As subsurface water moves downslope, it collects in topographically flatter convergent areas. The degree of convergence determines how much upslope area drains down to a given location. The slope of the flat areas affects the "ability" of water to move farther downslope. Soil hydraulic characteristics, hydraulic conductivity and soil depth, determine the transmissivity at a location and affect the ability of water to move farther downslope.

Soils and topographic parameters, watershed latitude, and a time series of precipitation and air temperature (table 1) must be specified to use TOPMODEL. The watershed latitude is used to generate a time series of day length that, along with the time series of temperature, is used to calculate potential evapotranspiration.

TOPMODEL predicts streamflow, estimates overland and subsurface flow, and estimates the depth to the water table. Overland flow for a given time step is calculated from the areal extent of the saturated land-surface areas and the precipitation intensity. Subsurface flow is computed as a function of the maximum subsurface-flow rate (determined by topographic and soils characteristics) and the watershed average depth to the water table. The watershed average depth to the water table is

computed by water balance; that is, by tracking input (precipitation) and output (overland flow, subsurface flow, and evapotranspiration).

If spatially distributed data on soil hydraulic characteristics are available, they can be used together with topographic data to simulate spatial patterns of saturated land-surface area development and spatial patterns of other hydrologic variables (table 1). If spatially distributed data on soil hydraulic characteristics are not available, a watershed average value can be specified along with the spatial distribution of topographic characteristics. The implication of the latter formulation on the model is that the location of zones within a watershed that are likely to produce overland flow is a function of spatial variability in topography, not in soil hydraulic characteristics.

## Differences Among Versions of TOPMODEL

Many versions of TOPMODEL, with varying levels of complexity, have been developed. The differences among versions of TOPMODEL can be grouped into two categories: (1) the level of spatial complexity and aggregation of the input and simulated processes; and (2) the specific processes represented in each version. The issue of spatial complexity will be addressed in later sections of this report.

The second category of differences among versions of TOPMODEL is the specific processes that are represented in each version. For example, some versions of TOPMODEL have snowmelt and snow-accumulation algorithms (Wolock and others, 1989), whereas others do not (Wood and others, 1988). Also, the same process may be simulated in all versions of the model but may be represented in different ways. Estimation of evapotranspiration rates, for example, varies considerably from one version of the model to another. In some versions, estimates of evapotranspiration are based on empirically derived values of potential evapotranspiration (Wolock and Hornberger, 1991), whereas others use physically based methods to compute evapotranspiration (Famiglietti, 1992).

The different versions of TOPMODEL do not include all the same concepts of streamflow-generation mechanisms. Some versions of

**Table 1. TOPMODEL input and output**

Input:	Time series of:	Precipitation Temperature Observed streamflow (for calibration)
	Topography	
	Spatial distributions of soil characteristics:	Hydraulic conductivity Depth to bedrock Depth of AB soil horizon Field capacity
	Latitude Area	
Output:	Time series of:	Total streamflow Subsurface flow
	Temporal and spatial distributions of:	Overland flow Depth to water table Saturated land-surface areas Soil moisture Evapotranspiration

TOPMODEL that have appeared in the literature simulate both the infiltration-excess overland flow concept and the variable-source-area concept of streamflow generation during precipitation events (Wood and others, 1990). Other versions of the model simulate only the variable-source-area concept (Wolock, 1988). All versions assume that streamflow during low-flow conditions is generated by drainage of water from the saturated subsurface zone into the stream channel (fig. 1).

## SIMULATING STREAMFLOW GENERATION WITH TOPMODEL

### TOPMODEL Equations

There are several components of TOPMODEL that describe different aspects of watershed hydrology. The model components explained in the following paragraphs simulate the variable-source-area concept of streamflow generation, snow accumulation and melt, evapotranspiration, streamflow generation from impervious areas, and channel routing of flow

from delivery to the stream through to the watershed outlet. Except for the variable-source-area concept of streamflow generation, these processes vary considerably from one published version of TOPMODEL to another and, in general, are treated simplistically in the version described in this report.

### Streamflow Generation

In the variable-source-area concept of streamflow generation, flow delivered to the stream channel from permeable parts of the watershed is estimated as the sum of saturation overland flow and subsurface flow, or:

$$q_{total} = q_{overland} + q_{subsurface} \quad (1)$$

where  $q_{total}$  [L/T] is the total flow per unit area,  $q_{overland}$  [L/T] is the saturation overland flow per unit area, and  $q_{subsurface}$  [L/T] is the subsurface flow per unit area (fig. 3). Saturation overland flow is the sum of direct precipitation on saturated areas and return flow, or:



$$q_{overland} = q_{direct} + q_{return}, \quad (2)$$

where  $q_{direct}$  [L/T] is direct precipitation on saturated areas, and  $q_{return}$  is return flow (fig. 2). Equations 1 and 2 can be combined to give:

$$q_{total} = q_{direct} + q_{return} + q_{subsurface}. \quad (3)$$

The starting points for deriving expressions to compute  $q_{direct}$ ,  $q_{return}$ , and  $q_{subsurface}$  are the continuity equation at some location  $x$  in the watershed and Darcy's Law. Assuming steady-state conditions with a spatially uniform recharge rate ( $R$ ) to the water table, continuity gives:

$$\text{Inflow to location } x = \text{Outflow from location } x, \quad (4)$$

or

$$A_x R = T_x \tan B_x C_x, \quad (5)$$

where  $A_x$  [L<sup>2</sup>] is the surface area upslope from  $x$  that drains past the location,  $T_x$  [L<sup>2</sup>/T] is the transmissivity of the saturated thickness at  $x$ ,  $\tan B_x$  is the hydraulic gradient at  $x$ , and  $C_x$  [L] is the contour width at  $x$  traversed by subsurface flow at the location (fig. 6).

The transmissivity of the saturated thickness at  $x$  is computed by assuming that saturated hydraulic conductivity [ $K_{(z)}$ ] decreases exponentially with depth  $z$  (measured positively in the downward direction) as:

$$K_{(z)} = K_0 e^{-fz}, \quad (6)$$

where  $K_0$  is the hydraulic conductivity at the soil surface, and  $f$  is a parameter that controls the rate of decrease with depth (fig. 7). The validity of this assumption is supported by data in Beven (1984) and Elsenbeer and others (1992).

Equation 6 is integrated over the saturated thickness from  $z_{wt}$  (the depth to the water table) to  $z_D$  (the total soil depth) to obtain  $T_x$  as:

$$T_x = \int_{z_{wt}}^{z_D} K_0 e^{-fz} dz, \quad (7)$$

or

$$T_x = \frac{K_0}{f} (e^{-fz_{wt}} - e^{-fz_D}). \quad (8)$$

Beven (1984) shows that typical values of  $f$  and  $z_D$  are large enough that equation 8 reduces to:

$$T_x = \frac{K_0}{f} (e^{-fz_{wt}}). \quad (9)$$

Equation 9 is substituted into equation 5 to get:

$$A_x R = \left( \frac{K_0}{f} e^{-fz_{wt}} \tan B \right)_x C_x. \quad (10)$$

Dividing by  $C_x$ , letting  $a_x = A_x/C_x$ ,  $T_0 = K_0/f$ , and solving for  $z_{wt}$  at location  $x$  gives:

$$z_{wt}(x) = -\frac{1}{f} \ln(R) - \frac{1}{f} \ln\left(\frac{a}{T_0 \tan B}\right)_x. \quad (11)$$

Integrating equation 11 over the entire watershed area to obtain  $\bar{z}_{wt}$ , the average depth to the water table, gives:

$$\bar{z}_{wt} = \frac{1}{A} \int_A z_{wt} dA, \quad (12)$$

or

$$\bar{z}_{wt} = -\frac{1}{f} \ln(R) - \frac{1}{f} \Lambda, \quad (13)$$

where  $\Lambda$  [ $\ln(T/L)$ ] is the areal average of  $\ln[a/(T_0 \tan B)]$ , given by:

$$\Lambda = \frac{1}{A} \int_A \ln\left(\frac{a}{T_0 \tan B}\right)_x dA. \quad (14)$$

Equation 13 is solved for  $(\ln R)/f$  and substituted into equation 11 to obtain an expression for  $z_{wt}$  at location  $x$  as a function of  $\bar{z}_{wt}$ :

$$z_{wt}(x) = \bar{z}_{wt} + \frac{1}{f} \left( \Lambda - \ln\left(\frac{a}{T_0 \tan B}\right)_x \right). \quad (15)$$

Traditionally, TOPMODEL equations are expressed in terms of the saturation deficit (denoted by  $S_x$  for the saturation deficit at location  $x$  and by  $\bar{S}$  for the watershed average saturation deficit). The saturation deficit is conceptually and mathematically equivalent to the depth to the water table multiplied by the readily drained soil porosity ( $n_{drain}$ ), or:

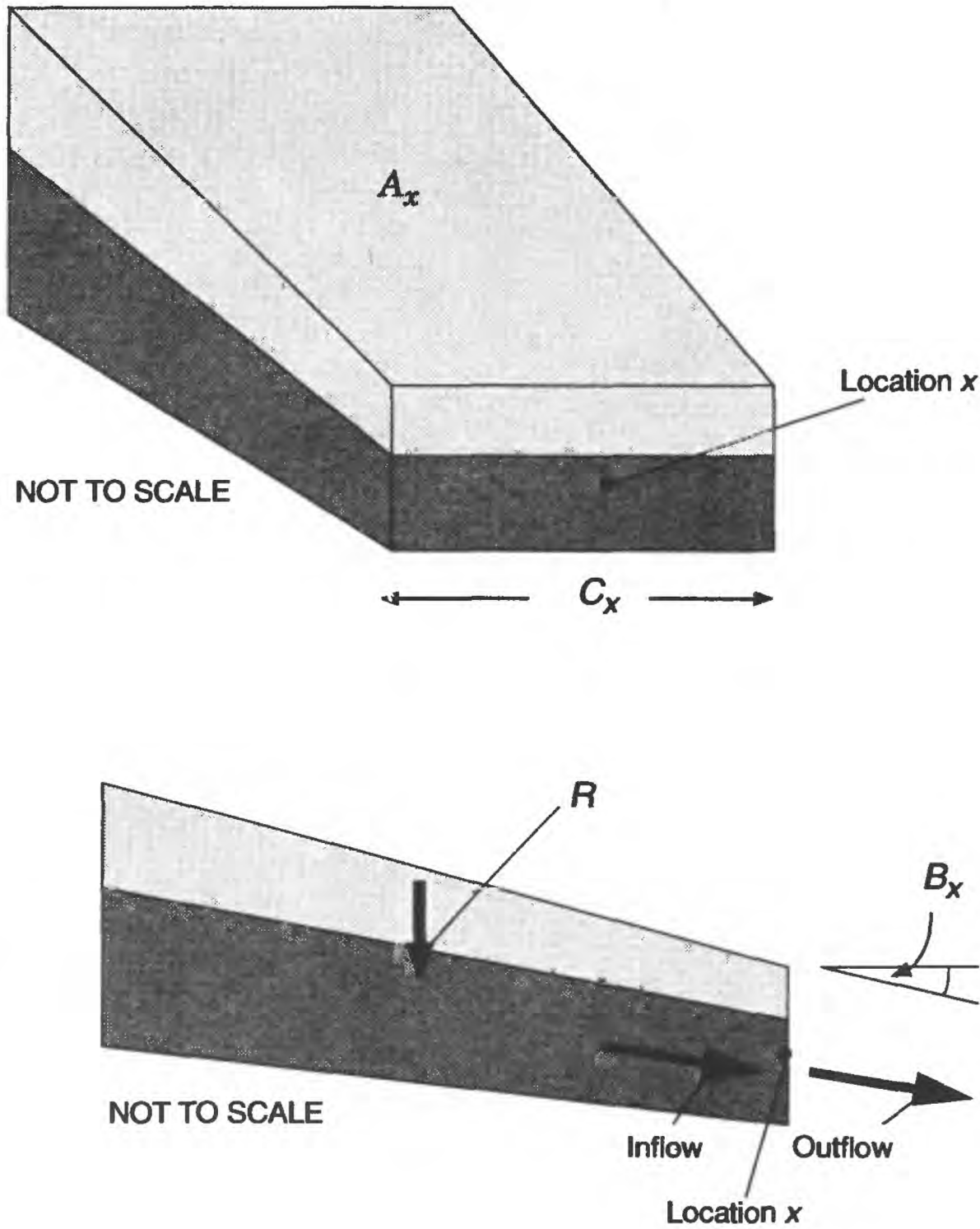


**Figure 6.** Definition of terms in the continuity equation for location  $x$ .  $A_x$  is the area upslope from  $x$  that drains past the location,  $C_x$  is the contour length at  $x$  traversed by subsurface flow at the location,  $R$  is the spatially uniform recharge rate, and  $B_x$  is the slope angle at  $x$ .

$$z_{wt} = S/n_{drain}. \quad (16)$$

$$m = n_{drain}/f. \quad (18)$$

Making this substitution into equation 15 and multiplying by  $n_{drain}$  gives:

$$S_x = \bar{S} + \frac{n_{drain}}{f} \left( \Lambda - \ln \left( \frac{a}{T_0 \tan B} \right)_x \right). \quad (17)$$

Another traditional TOPMODEL convention is to define a scaling parameter  $m$  such that:

Equation 17 then becomes:

$$S_x = \bar{S} + m \left[ \Lambda - \ln \left( \frac{a}{T_0 \tan B} \right)_x \right]. \quad (19)$$

Equation 19 states that the saturation deficit at any location  $x$  is determined by the watershed average saturation deficit ( $\bar{S}$ ) and the difference between the mean of the  $\ln [a/(T_0 \tan B)]$  distribution ( $\Lambda$ ) and the value



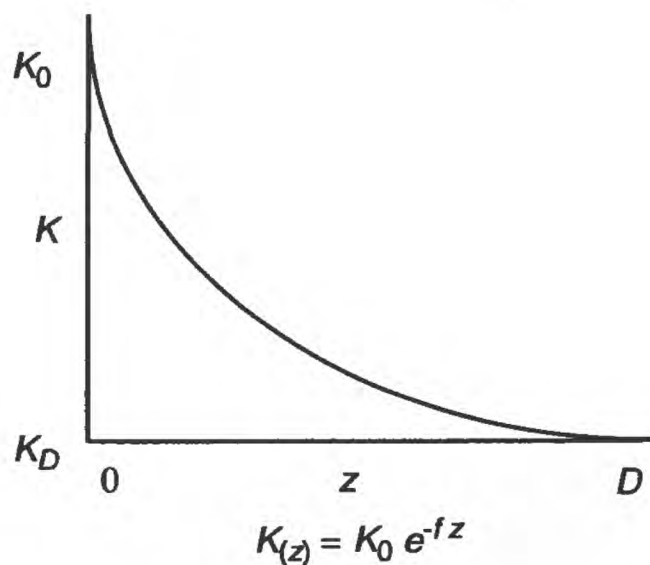


**Figure 7.** Relation between saturated hydraulic conductivity ( $K$ ) and soil depth ( $z$ ).  $K_0$  is saturated hydraulic conductivity at the soil surface ( $z=0$ ),  $K_D$  is saturated hydraulic conductivity at the depth to bedrock ( $z=D$ ), and  $f$  is the parameter that controls the rate of change of saturated hydraulic conductivity with changing soil depth.

of  $\ln [a/(T_0 \tan B)]$  at location  $x$ . Large values of  $\ln [a/(T_0 \tan B)]$  indicate the locations within a watershed most likely to be saturated and produce overland flow. These locations are topographically convergent and have gentle slopes and low transmissivity; that is, they drain a significant upslope area of the watershed and have limited capacity to conduct water from the drained area in a downslope direction. The scaling parameter  $m$  in equation 19 affects the range of variability in the saturation deficit over the watershed given the  $\ln [a/(T_0 \tan B)]$  distribution.

Equation 19 is used to determine  $q_{direct}$  and  $q_{return}$ . Any location  $x$  in the watershed where  $S_x \leq 0$  is saturated and has the potential to produce saturation overland flow; any location where  $S_x < 0$  produces return flow. The values of  $q_{direct}$  and  $q_{return}$  are determined by computing  $S_x$  for every location in the watershed and then determining  $a_x$ , the area of every location where  $S_x \leq 0$ .

The value of  $q_{direct}$  is computed by summing the products of the saturated areas,  $a_x$ , multiplied by the precipitation intensity,  $i$ , and dividing by the watershed area,  $A$ , as:

$$q_{direct} = \frac{\sum a_x i}{A} \quad \text{where } S_x \leq 0. \quad (20)$$

The value of  $q_{return}$  is computed by summing the products of the saturated areas multiplied by the absolute value of the negatively valued saturation deficits, as:

$$q_{return} = \frac{\sum a_x |S_x|}{A} \quad \text{where } S_x < 0. \quad (21)$$

Equation 19 shows that the parameter  $m$ , the variable  $\bar{S}$ , and the distribution of  $\ln [a/(T_0 \tan B)]$  need to be determined to calculate  $S_x$ . The  $\ln [a/(T_0 \tan B)]$  distribution can be derived from observed topographic and soil hydraulic information. The scaling parameter  $m$  can be derived from soil information using equation 18 or treated as a calibrated parameter. The value of  $\bar{S}$  is initialized at the beginning of a simulation to an arbitrary value, and then the rate of change of  $\bar{S}$  over time ( $t$ ) is given by:

$$\frac{d\bar{S}}{dt} = -q_{drain} + q_{subsurface}, \quad (22)$$

where  $q_{subsurface}$  is subsurface flow, and  $q_{drain}$  [ $L/T$ ] is the flux of water that drains from the upper soil horizon to the saturated subsurface zone. The drainage flux,  $q_{drain}$ , is estimated as:

$$q_{drain} = \frac{K w_{drain}}{S_x}, \quad (23)$$

where  $K$  [ $L/T$ ] is the saturated hydraulic conductivity of the C horizon (the unconsolidated zone) of the soil,  $w_{drain}$  [ $L$ ] is the amount of water available for drainage, and  $S_x$  is a positive valued saturation deficit. When  $S_x$  is less than or equal to zero,  $q_{drain}$  is set to zero.

The rate of change in the quantity of water available for drainage ( $w_{drain}$ ) over time ( $t$ ) is given by:

$$\frac{dw_{drain}}{dt} = ex_{et} + q_{macro} - q_{drain}, \quad (24)$$

where  $ex_{et}$  [ $L/T$ ] is the amount of precipitation in excess of evapotranspiration demand and field-capacity storage, and  $q_{macro}$  [ $L/T$ ] is

precipitation that bypasses field-capacity storage. The macropore flow ( $q_{macro}$ ) is estimated as:

$$q_{macro} = p_{macro} i, \quad (25)$$

where  $p_{macro}$  [fraction] is a parameter representing the proportion of precipitation input ( $i$ ) that bypasses the soil compartment exposed to evapotranspiration and becomes available to decrease the saturation deficit. The parameter  $p_{macro}$  can be set to an assumed value based on the modeler's knowledge of the watershed soils or treated as a calibrated parameter.

Subsurface flow,  $q_{subsurface}$ , is computed by combining Darcy's Law for saturated subsurface flux ( $q_x$ ) (the right-hand side of equation 5 divided by  $C_x$ ) with equation 9, the expression for transmissivity of the saturated thickness, along with equations 16 and 18 to get:

$$q_x = (T_0 \tan B)_x e^{-\frac{S_x}{m}}. \quad (26)$$

Equation 26 is integrated along the lengths of all stream channels to compute the total subsurface flow delivered to the stream and divided by the watershed area to get:

$$q_{subsurface} = \frac{\int_L (T_0 \tan B)_x e^{-\frac{S_x}{m}} dL}{A}, \quad (27)$$

or

$$q_{subsurface} = e^{-\Lambda} e^{-\frac{\bar{S}}{m}}, \quad (28)$$

where  $\Lambda$  is the areal mean value of  $\ln [a/(T_0 \tan B)]$ .

A final change of variables to match the traditional notation in TOPMODEL is to let:

$$q_{submax} = e^{-\Lambda}. \quad (29)$$

Combining equations 28 and 29 then gives the expression:

$$q_{subsurface} = q_{submax} e^{-\frac{\bar{S}}{m}}. \quad (30)$$

## Spatial Aggregation

A variation of the derivation just given is required when the spatial distribution of  $T_0$  is not known, as is often the case. In this formulation, an average value of  $T_0$  is used in TOPMODEL, assuming that  $T_0$  is not variable over the area of the watershed. The alternative derivation results in the expression for the saturation deficit at location  $x$  as:

$$S_x = \bar{S} + m \left[ \lambda - \ln \left( \frac{a}{\tan B} \right)_x \right], \quad (31)$$

where all the terms are as before, except for  $\lambda$  [ $\ln(L)$ ] which is now the watershed average value of the  $\ln(a/\tan B)$  distribution. This formulation of TOPMODEL implies that it is only the spatial variation in topography that determines variability in the saturation deficit over the watershed.

Values of  $\ln(a/\tan B)$  relate directly to the topographic likelihood of development of saturated, overland-flow producing areas [that is, smaller values of  $\ln(a/\tan B)$  indicate less potential for development of saturation]. Large values of  $\ln(a/\tan B)$  occur at locations where large upslope areas are drained (high value of  $a$ ) and the local slope is gentle (low value of  $\tan B$ ). The relation of  $\ln(a/\tan B)$  to saturated source-area development is evident when the spatial distribution is displayed graphically. Figure 8, for example, shows a graphical representation of the elevation and  $\ln(a/\tan B)$  distributions for a subbasin of the Sleepers River watershed in Vermont. The light areas on the  $\ln(a/\tan B)$  figure have the largest values and are the most likely to become saturated.

When equation 31 is used instead of equation 19 to estimate the saturation deficit, the maximum subsurface flow rate used in equation 30 now should be:

$$q_{submax} = T_0 e^{-\lambda}. \quad (32)$$

All the other equations that comprise TOPMODEL are unchanged.

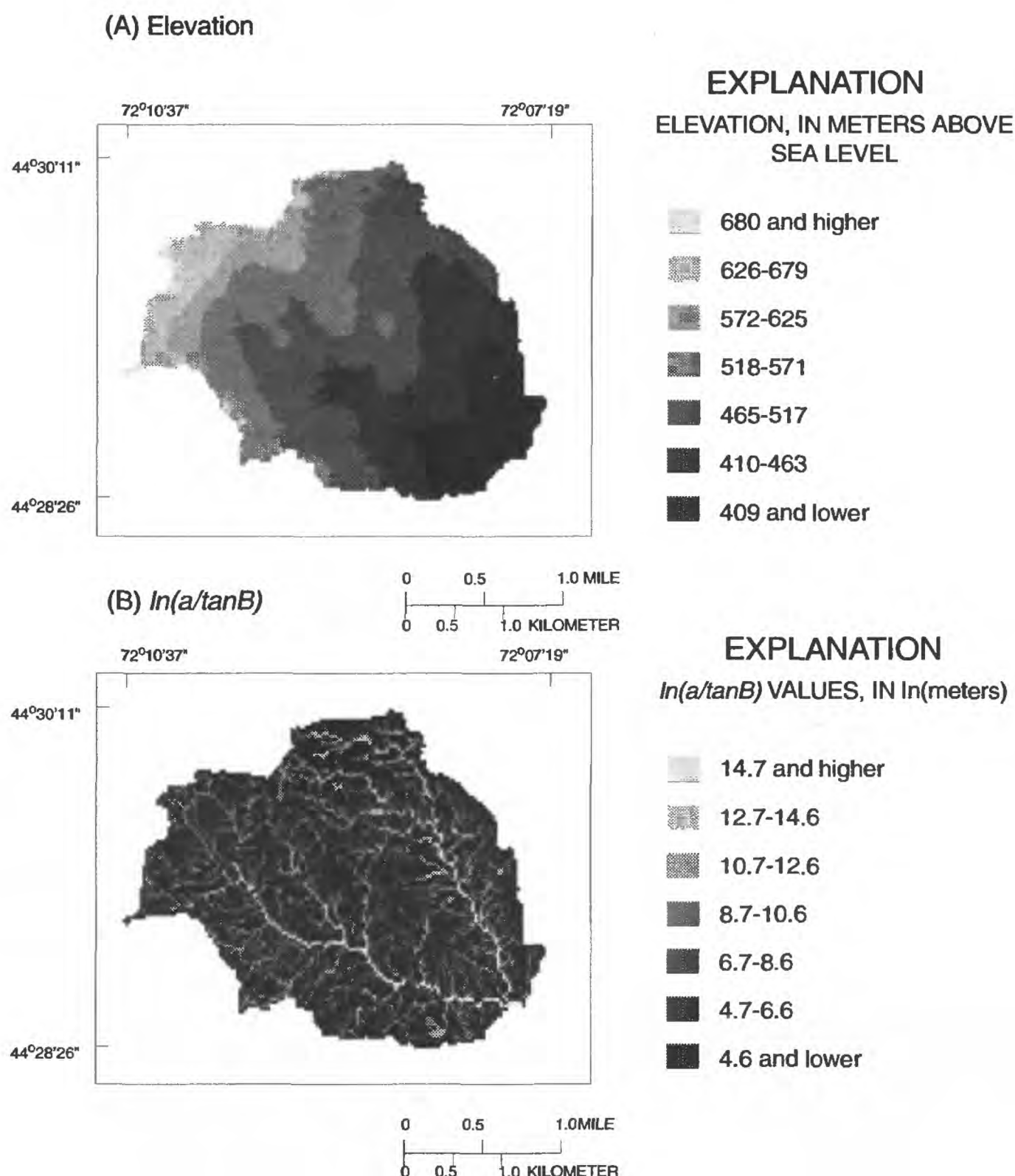


**Figure 8.** (A) elevation and (B)  $\ln(a/\tan B)$  values for subbasin W-3 in Sleepers River watershed in Vermont.

One simplifying assumption that decreases computational time in using the model is that all locations in the watershed with the same  $\ln(a/\tan B)$  or  $\ln[a/(T_0 \tan B)]$  value (depending on whether the spatial distribution of  $T_0$  is known) are hydrologically similar in their response. This assumption allows the aggregation of the  $\ln(a/\tan B)$  or  $\ln[a/(T_0 \tan B)]$  distribution from a spatially explicit description of the watershed into one of intervals in  $\ln(a/\tan B)$  or  $\ln[a/(T_0 \tan B)]$  (fig. 9). The model equations do not change, but the calcula-

tions are performed using the  $\ln(a/\tan B)$  or  $\ln[a/(T_0 \tan B)]$  values of frequency-distribution interval midpoints instead of the individual spatially distributed values. By knowing the relative frequency (that is, the proportion of watershed area) corresponding to each interval midpoint, total watershed values for the model variables can be calculated. TOPMODEL can be used in the true spatial domain (as in Wood and others, 1990) or in the frequency domain (as in Wolock and others, 1990).



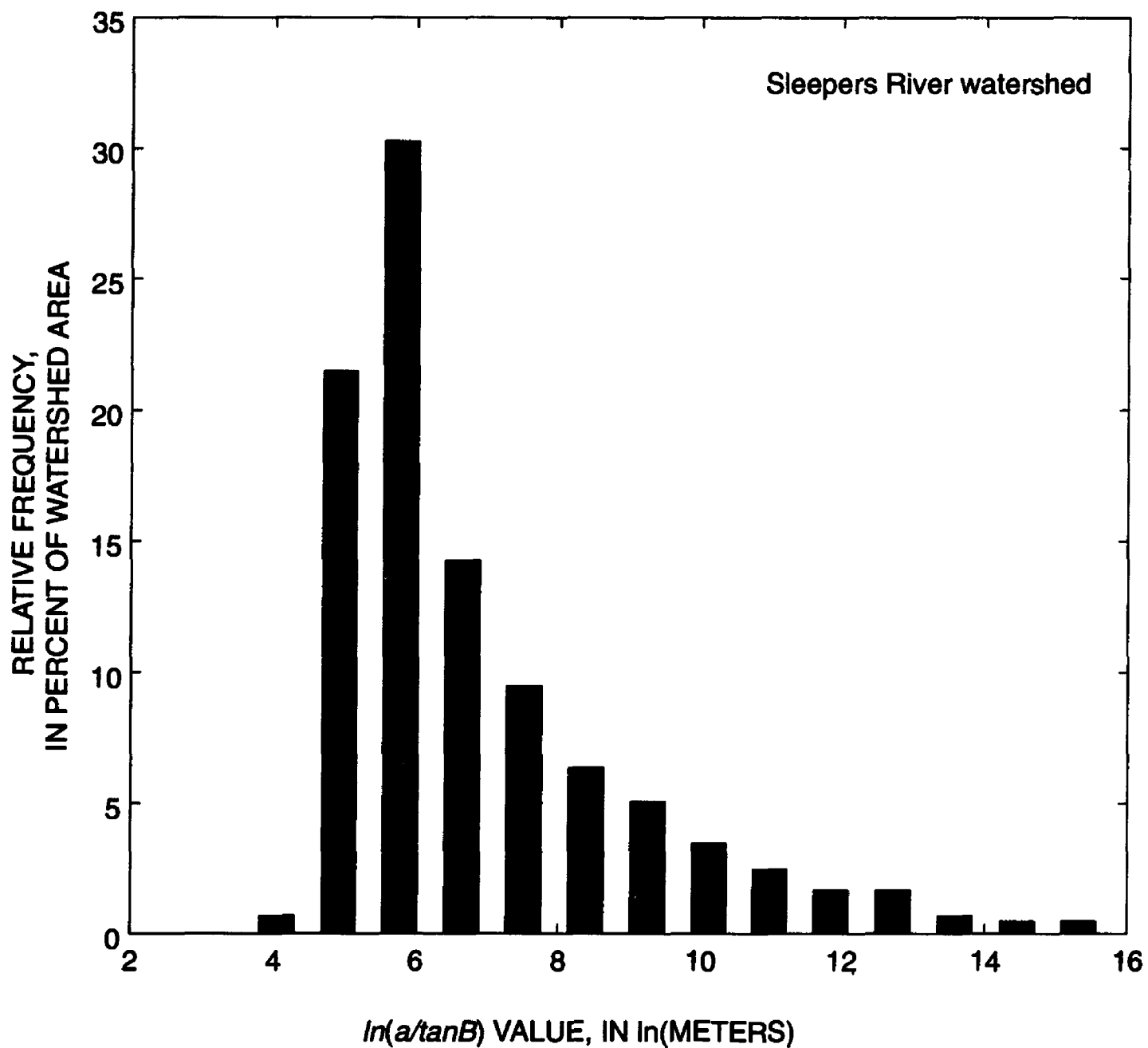


**Figure 9.** Relative frequency distribution of  $\ln(a/\tan B)$  values for Sleepers River watershed in Vermont.

### Snow Accumulation and Melt

Precipitation is the main forcing function of TOPMODEL. Whether it falls as rain or snow and the rate at which accumulated snow melts are simulated using a simple method similar to one developed by the U.S. Army Corps of Engineers (U.S. Corps of Engineers, 1960; Chow, 1964). Snow accumulation occurs when the observed air temperature ( $Temp$  [deg]) is less than a specified temperature cutoff value ( $T_{cut}$  [deg]). The value of  $T_{cut}$  depends on the vegetative cover, slope, and aspect of the site, and suggested values are given in the literature (for example, see Chow, 1964).  $T_{cut}$  also can be treated as a calibrated parameter because a watershed is a collection of diverse sites and only a single value of precipitation intensity is used for the entire watershed.

Snow melts when the air temperature is above  $T_{cut}$ . The rate at which it melts depends on the air temperature and whether it is raining. In the absence of rain, the maximum depth of snowmelt ( $d_{melt}$  [L]) is estimated as:

$$d_{melt} = p_{snow} (Temp - T_{cut}) , \quad (33)$$

where  $p_{snow}$  [L/deg] is a parameter that can be set at a "universal" constant or calibrated to observed data. If rain occurs, the maximum depth of snowmelt is given as:

$$d_{melt} = p_{rain} i (Temp - T_{cut}) , \quad (34)$$

where  $p_{rain}$  [1/deg] is a parameter that can be set or calibrated, and  $i$  [L] is the depth of rain that falls.

## Evapotranspiration

Evapotranspiration ( $ET$ ) is a function of both the potential rate (the rate  $ET$  would occur if unlimited water were available) and the actual amount of water that is available. Potential evapotranspiration ( $PET$ ) is calculated using the Hamon formula (Hamon, 1961). This is an empirical relationship of the form:

$$PET = CD^2\rho, \quad (35)$$

where  $C [L^4/(mT^2)]$  is an empirical constant,  $D [T]$  is the maximum possible clear-sky duration of sunshine, and  $\rho [m/L^3]$  is the mass density of water in air, a function of air temperature.  $D$  is estimated from watershed latitude by calculating the solar declination and the sunset-hour angle (Keith and Kreider, 1978).

It is assumed that evapotranspiration depletes water from the root zone of the soil at its potential rate until the root-zone water storage is depleted. The maximum root-zone water storage ( $D_{root} [L]$ ) is estimated as:

$$D_{root} = z_{root}\theta_{fc}, \quad (36)$$

where  $z_{root} [L]$  is the root-zone depth, and  $\theta_{fc} [L^3/L^3]$  is the field capacity of the soil.

## Impervious Areas

The contribution of impervious areas to streamflow ( $q_{imp}$ ) is computed simply as:

$$q_{imp} = p_{imp} i, \quad (37)$$

where  $p_{imp} [fraction]$  is the proportion of the total watershed area that is impervious, and  $i [L]$  is the precipitation depth.

## Channel Routing

After water flows into the stream channel as pervious-area flow ( $q_{total}$  from equation 3) and/or impervious-area flow ( $q_{imp}$  from equation 37), it is routed through the channel system to the stream outlet. Routing is accomplished with the following simple algorithm. First, the number of time steps ( $t_{steps} [T]$ ) required for all the water delivered to the channel during a given time step to reach the outlet is estimated as:

$$t_{steps} = \frac{d_{max}}{v}, \quad (38)$$

where  $d_{max} [L]$  is the longest channel distance upstream from the outlet, and  $v [L/T]$  is an estimate of the velocity of the flow in the channel. Next, the total flow in a given time step is divided by the number of time steps required for all the water to reach the outlet:

$$q_{portion} = \frac{q_{total} + q_{imp}}{t_{steps}} \quad (39)$$

to give the portion of flow reaching the channel outlet in one time step ( $q_{portion} [L]$ ). Thus, the sum of  $q_{total}$  and  $q_{imp}$  is partitioned into  $t_{steps}$  portions, requiring a total of  $t_{steps}$  time steps for all the flow to exit the watershed.

## Setting Model Parameters

Many model-parameter values, such as the  $\ln(a/\tan B)$  or  $\ln[a/(T_0 \tan B)]$  distribution, can be set from available information on watershed characteristics. Other parameters, such as  $m$  (the scaling parameter) and  $p_{macro}$  (the proportion of precipitation input that bypasses the soil compartment), usually must be derived through model calibration because the information required to set their values is not readily measurable. This section of the report describes methods for setting soil-hydraulic and topographic parameter values from readily observed watershed characteristics. A later section describes a parameter-calibration method that can be used to determine values for parameters that cannot be readily set.

## Soil Hydraulic Parameters

Onsite measurements of saturated hydraulic conductivity and soil depth are preferred over values inferred from a soil survey. In the absence of measured data, however, soil-survey data can be used to estimate field capacity, saturated hydraulic conductivity, and soil depth. Soil depth usually is given in a soil survey, as well as soil textural information, from which field capacity and saturated hydraulic conductivity can be estimated (Cosby and others, 1984). By knowing the percentage of sand ( $p_{sand}$ ), saturated hydraulic conductivity

( $K$ ) can be estimated from the regression equation given by Cosby and others (1984):

$$\log K = -0.884 + 0.0153 p_{sand}, \quad (40)$$

where  $\log$  is the base 10 logarithm, and the units of  $K$  are inches per hour.

$K$  is multiplied by soil depth,  $z$ , to compute  $T_0$ . It is assumed that the value of  $K$  computed in equation 40 represents the hydraulic conductivity of the C horizon of the soil. It is further assumed that the hydraulic conductivity of the AB horizon (the eluvial and illuvial zones) is two orders of magnitude greater than the conductivity of the C horizon. (This is a very crude approximation of equation 6.) Therefore, the saturated hydraulic transmissivity of the soil profile ( $T_0$ ) is calculated as:

$$T_0 = z_{ab} 100 K + z_c K, \quad (41)$$

where  $z_{ab}$  [L] is the thickness of the AB horizon, and  $z_c$  [L] is the thickness of the C horizon. Values for  $z_{ab}$  and  $z_c$  usually are available from soil surveys.

Given  $p_{sand}$  and percent clay ( $p_{clay}$ ), the parameters of the moisture retention curve given by:

$$\phi = \phi_{sat} \left( \frac{\theta}{\theta_{sat}} \right)^{-b} \quad (42)$$

can be derived, where  $\phi$  is matric potential [centimeters of water],  $\phi_{sat}$  is matric potential at saturation [centimeters of water],  $\theta$  is volumetric water content [percent],  $\theta_{sat}$  is volumetric water

content at saturation [percent], and  $b$  is the slope of the retention curve on a logarithmic plot. The parameters are estimated as:

$$\log(\phi_{sat}) = 1.88 - 0.0131 p_{sand}, \quad (43)$$

$$\theta_{sat} = 48.9 - 0.126 p_{sand}, \quad (44)$$

and

$$b = 2.91 + 0.159 p_{clay}. \quad (45)$$

By definition,  $\phi$  at field capacity is 334 centimeters. Substituting this value in equation 42, the equation can be solved for  $\theta$  at field capacity.

### Spatial Distribution of $\ln(a/\tan B)$

The spatial distribution of  $\ln(a/\tan B)$  can be used in TOPMODEL directly or can be used to compute a frequency distribution. The spatial distribution is computed from a grid of elevations. (The grid also is referred to as a "sheet" or "map.") The instructions that follow are for a set of programs written by S.K. Jenson (TGS Technology, Inc., EROS Data Center, Sioux Falls, S. Dak.) or modified versions of her programs. (For more information about how these programs work, see Jenson and Domingue, 1988.) Table 2 lists the program names and functions.

The programs operate on 2-byte (*integer\*2*) and 4-byte (*integer\*4*) binary, direct-access files. The Fortran OPEN statements in the programs need to be checked to make sure that they have the correct record length. The correct record

**Table 2.** Programs used to compute the  $\ln(a/\tan B)$  distribution and moments

Program	Description	Input file names	Output file names
concave	Remove depressions from the elevation data.	ele	ele
direct	Determine steepest downslope directions.	ele	dir
count	Compute number of upslope cells.	dir	num
slope	Compute values of $\tan B$ in steepest downslope direction.	ele, dir	slo
atanb	Compute $\ln(a/\tan B)$ spatial distribution.	num, slo	atn
atnmom	Compute moments of the $\ln(a/\tan B)$ distribution.	atn	None

length depends on the word length of an *integer\*2* variable, which varies among types of computers.

The arrangement of elevations in the file must be as if viewed from above (a plan view). The first sample (=column) of the first line (=row) is the elevation point in the upper left corner of the map. If the line and sample dimensions of the grid are *nl* by *ns*, then the file is *nl* lines long, and each line contains *ns* data samples.

The steps in data processing are as follows:

1. The depressions in the elevation data are filled using a program called **concave** so that a downslope path exists for all points to flow off the edges of the map (fig. 10). A depression is a point with an elevation value lower than all of its neighboring points. The file of elevations (both pre- and post-modification) is an *integer\*2* file called **ele** in the example below.
2. The elevation at each point is compared to the elevations of its
- neighboring points using a program called **direct**, which assigns the steepest downslope direction to each point on the map (fig. 11). Locations along the perimeter of the map are automatically assigned the directions that force flow off the edges of the map. The input file of elevations is called **ele**, and the *integer\*2* output file of directions is called **dir**.
3. The number of points upslope from each point (number of uphill points that drain into a given point) are calculated (fig. 12) using the program called **count**. The input file of directions is called **dir**, and the output file of upslope point counts is an *integer\*4* file called **num**.
4. The magnitude of the slope in the steepest downslope direction is calculated (fig. 13) using the program called **slope**. The input files are **ele** and **dir**, and the output file is an *integer\*2* file called **slo**. The values in **slo** are values of *tanB* multiplied by 1,000. This allows numbers with three digits to the right of the decimal

(A) Elevation data before using the program concave.

495	497	499	502	503	507	510	514	522	525
497	499	501	504	508	512	515	518	527	529
502	505	506	505	508	513	515	519	526	532
508	510	511	510	511	514	514	518	524	530
514	516	516	516	<b>509</b>	519	519	522	525	530
517	522	522	521	521	524	523	522	522	526
518	520	521	519	524	526	523	523	521	520
516	519	519	519	524	528	524	519	516	514
518	521	519	519	522	526	522	517	512	510
515	522	524	522	524	521	521	514	510	513

(B) Elevation data after using the program concave.

495	497	499	502	503	507	510	514	522	525
497	499	501	504	508	512	515	518	527	529
502	505	506	505	508	513	515	519	526	532
508	510	511	510	511	514	514	518	524	530
514	516	516	516	<b>510</b>	519	519	522	525	530
517	522	522	521	521	524	523	522	522	526
518	520	521	519	524	526	523	523	521	520
516	519	519	519	524	528	524	519	516	514
518	521	519	519	522	526	522	517	512	510
515	522	524	522	524	521	521	514	510	513

**Figure 10.** (A) elevation grid file containing a depression highlighted in bold and (B) same elevation file with the depression removed after using the program concave.



(A) Elevation data after using the program concave.

495	497	499	502	503	507	510	514	522	525
497	499	501	504	508	512	515	518	527	529
502	505	506	505	508	513	515	519	526	532
508	510	511	510	511	514	514	518	524	530
514	516	516	516	510	519	519	522	525	530
517	522	522	521	521	524	523	522	522	526
518	520	521	519	524	526	523	523	521	520
516	519	519	519	524	528	524	519	516	514
518	521	519	519	522	526	522	517	512	510
515	522	524	522	524	521	521	514	510	513

(B) Downslope directions.

32	128	128	128	128	128	128	128	128	128
32	64	64	64	128	64	64	64	64	2
32	128	128	64	32	32	64	32	32	2
32	64	128	128	64	64	64	32	32	2
32	128	128	128	64	32	128	64	64	2
32	128	128	1	128	64	128	64	4	2
32	16	8	8	32	64	4	4	8	2
32	32	32	32	32	16	2	4	4	2
32	16	128	64	32	8	4	2	8	2
32	8	8	8	8	8	8	8	8	2

(C) Graphical representation of downslope directions.

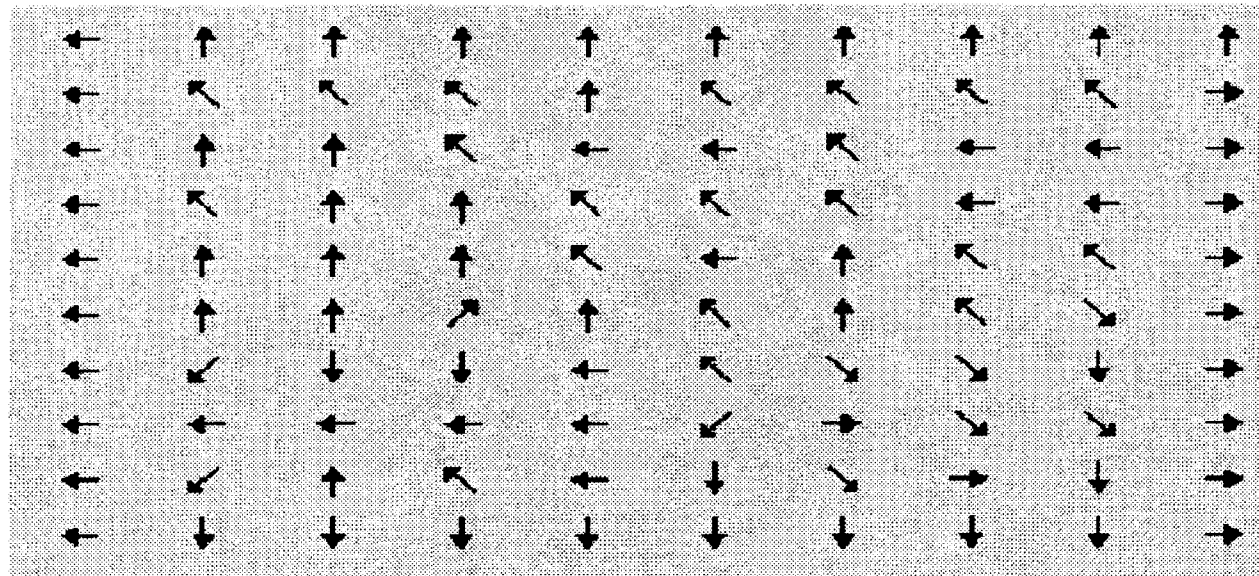


**Figure 11.** (A) elevation grid file containing no depressions, (B) grid of downslope directions produced by the program direct, and (C) graphical representation of downslope directions. The downslope-direction values correspond to the following angles, measured clockwise from the top: 1=45°, 2=90°, 4=135°, 8=180°, 16=225°, 32=270°, 64=315°, and 128=360°

place to be stored as integers in an *integer\*2* file. Values of  $\tan B$  are not computed along the perimeter of the map and automatically are assigned a missing-value flag of -1.

5. The  $\ln(a/\tan B)$  values are calculated (fig. 14) using the program called **atanb**. The input files are **num** and **slo**, and the output is an *integer\*2* file

called **atn**. The values in **atn** are values of  $\ln(a/\tan B)$  multiplied by 100. This allows numbers with two digits to the right of the decimal place to be stored in an *integer\*2* file. Missing values are denoted by large negative numbers and occur where  $\tan B$  is not calculated at the edge of the map.

(A) Downslope directions.

32	128	128	128	128	128	128	128	128	128
32	64	64	64	128	64	64	64	64	2
32	128	128	64	32	32	64	32	32	2
32	64	128	128	64	64	64	32	32	2
32	128	128	128	64	32	128	64	64	2
32	128	128	1	128	64	128	64	4	2
32	16	8	8	32	64	4	4	8	2
32	32	32	32	32	16	2	4	4	2
32	16	128	64	32	8	4	2	8	2
32	8	8	8	8	8	8	8	8	2

(B) Number of upslope nodes.

2	26	1	0	5	1	1	1	0	0
0	1	25	0	0	3	0	0	0	0
3	0	3	20	10	8	2	1	0	0
0	2	2	7	0	0	7	2	0	0
0	1	1	0	5	0	2	0	0	0
0	0	0	0	1	0	0	0	0	0
0	0	0	1	0	0	0	0	0	1
12	10	9	3	0	0	0	2	2	0
0	0	0	2	1	0	0	0	4	3
1	0	0	0	0	1	0	1	5	0

**Figure 12.** (A) grid of downslope directions produced by the program **direct** and (B) grid of number of upslope nodes. The downslope-direction values correspond to the following angles, measured clockwise from the top: 1=45°, 2=90°, 4=135°, 8=180°, 16=225°, 32=270°, 64=315°, and 128=360°.

6. The moments of the  $\ln(a/\tan B)$  spatial distribution are computed using the program **atnmom**. The input file is **atn**, and the output is listed to the console.

Step-by-step instructions are given below for computing the spatial distribution of  $\ln(a/\tan B)$ . Information that the user enters is printed in bold. *nl* is the number of lines (*nl*=10 in the example), and *ns* is the number of samples (*ns*=10 in the example) in the data file. The example is executed on a Data General AViiON<sup>1</sup> workstation.

1. Use the program **concave** to remove the depressions from the elevation data. BOXNL and BOXNS define the size of the moving data window being processed by the program at any given time. OVERLAP sets the overlap in the position of the window relative to its previous position as it moves. After the user provides the required input, messages showing the

movement of the processing window are written to the console.

```
>concave
ENTER NL, NS, BOXNL,
BOXNS, OVERLAP, ELEV
FILE
10
10
5
5
3
ele
INIT COMPLETE FOR 1 1
0 POLYGON PARTS
BIGPASS 1
INIT COMPLETE FOR 1 3
0 POLYGON PARTS
BIGPASS 2
INIT COMPLETE FOR 1 5
0 POLYGON PARTS
BIGPASS 3
.
.
.
INIT COMPLETE FOR 9 9
0 POLYGON PARTS
BIGPASS 26
```

<sup>1</sup>The use of brand names in this report is for identification purposes only and does not constitute endorsement by the U.S. Geological Survey.

(A) Elevation data after running the program concave.

495	497	499	502	503	507	510	514	522	525
497	499	501	504	508	512	515	518	527	529
502	505	506	505	508	513	515	519	526	532
508	510	511	510	511	514	514	518	524	530
514	516	516	516	510	519	519	522	525	530
517	522	522	521	521	524	523	522	522	526
518	520	521	519	524	526	523	523	521	520
516	519	519	519	524	528	524	519	516	514
518	521	519	519	522	526	522	517	512	510
515	522	524	522	524	521	521	514	510	513

(B) Downslope directions.

32	128	128	128	128	128	128	128	128	128
32	64	64	64	128	64	64	64	64	2
32	128	128	64	32	32	64	32	32	2
32	64	128	128	64	64	64	32	32	2
32	128	128	128	64	32	128	64	64	2
32	128	128	1	128	64	128	64	4	2
32	16	8	8	32	64	4	4	8	2
32	32	32	32	32	16	2	4	4	2
32	16	128	64	32	8	4	2	8	2
32	8	8	8	8	8	8	8	8	2

(C)  $\tan B$  values.

-1	-1	-1	-1	-1	-1	-1	-1	-1	-1
-1	100	100	133	167	200	200	200	300	-1
-1	200	167	100	100	167	67	133	233	-1
-1	200	167	167	133	133	33	133	200	-1
-1	200	167	200	0	300	167	200	167	-1
-1	200	200	267	367	333	133	67	33	-1
-1	100	67	0	167	133	100	167	167	-1
-1	100	0	0	167	133	167	167	133	-1
-1	133	0	0	100	167	200	167	67	-1
-1	-1	-1	-1	-1	-1	-1	-1	-1	-1

**Figure 13.** (A) grid of elevations, (B) grid of steepest downslope directions, and (C) grid of  $\tan B$  values (multiplied by 1,000). The  $\tan B$  values are set to -1 along the perimeter of the grid.

- Use the program **direct** to calculate the steepest downslope direction. If a new **dir** file is being created by the program, enter 0 when prompted for the RESTART code. Specify the RESTART code to 1 if the **dir** file already exists but is being modified by the program. After providing the required input, user messages showing the movement of the processing window are written to the console.

```
>direct
ENTER NL,NS,CODE 1 TO
RESTART,ELEV FILE,DIR
FILE
10
```

```
10
0
ele
dir
DOWNWARD PASS 1FIRSTL
2LASTL 9
UPWARD PASS 2FIRSTL
7LASTL 7
```

- Use the program **count** to calculate the number of upslope nodes. If a new **num** file is being created by the program, enter 0 when prompted for the RESTART code. Specify the RESTART code to 1 if the **num** file already exists but is being modified by the program. After providing the

(A) Number of upslope nodes.

2	26	1	0	5	1	1	1	0	0
0	1	25	0	0	3	0	0	0	0
3	0	3	20	10	8	2	1	0	0
0	2	2	7	0	0	7	2	0	0
0	1	1	0	5	0	2	0	0	0
0	0	0	0	1	0	0	0	0	0
0	0	0	1	0	0	0	0	0	1
12	10	9	3	0	0	0	2	2	0
0	0	0	2	1	0	0	0	4	3
1	0	0	0	0	1	0	1	5	0

(B)  $\tan B$  values.

-1	-1	-1	-1	-1	-1	-1	-1	-1	-1
-1	100	100	133	167	200	200	200	300	-1
-1	200	167	100	100	167	67	133	233	-1
-1	200	167	167	133	133	33	133	200	-1
-1	200	167	200	0	300	167	200	167	-1
-1	200	200	267	367	333	133	67	33	-1
-1	100	67	0	167	133	100	167	167	-1
-1	100	0	0	167	133	167	167	133	-1
-1	133	0	0	100	167	200	167	67	-1
-1	-1	-1	-1	-1	-1	-1	-1	-1	-1

(C)  $\ln(a/\tan B)$  values.

-999	-999	-999	-999	-999	-999	-999	-999	-999	-999
-999	640	896	542	519	640	501	501	461	-999
-999	501	658	875	810	739	720	611	486	-999
-999	611	629	727	542	542	889	652	501	-999
-999	570	588	501	927	461	629	501	519	-999
-999	501	501	472	510	450	542	610	681	-999
-999	570	610	817	519	542	570	519	519	-999
-999	810	978	886	519	542	519	629	652	-999
-999	542	748	857	640	519	501	519	771	-999
-999	-999	-999	-999	-999	-999	-999	-999	-999	-999

**Figure 14.** (A) grid of number of upslope nodes, (B) grid of  $\tan B$  values (multiplied by 1,000), and (C) grid of  $\ln(a/\tan B)$  values (multiplied by 100). The  $\tan B$  values are set to -1 along the perimeter of the grid. In computing  $\ln(a/\tan B)$  for points where  $\tan B$  equals 0, the  $\tan B$  value is reset to  $0.5/(\text{spacing})$ , where  $\text{spacing}$  is the distance between adjacent grid nodes.

required input, user messages  
showing the movement of the  
processing window are written to the  
console.

```
>count
ENTER NL,NS,CODE 1 TO
RESTART,DIR FILE,COUNT
FILE
10
10
0
dir
num
```

```
DOWNWARD PASS 1
UPWARD PASS 2
DOWNWARD PASS 3
```

4. Use the program **slope** to calculate the slope in the steepest downslope direction. The grid spacing is the distance between adjacent elevation points and needs to be in the same units of length as the elevation data. The output file, called **slo**, is an *integer\*2* file containing the  $\tan B$  values multiplied by 1,000, which allows numbers with three digits to

the right of the decimal place to be stored in an integer format. Values of  $\tan B$  are not calculated along the edge of the map and are assigned a missing-value flag of -1.

```
>slope
ENTER NL,NS,DIR
FILE,ELEV FILE,SLOPE FILE
10
10
dir
ele
slo
GIVE THE GRID SPACING:
30
```

5. Use the program **atanb** to calculate  $\ln(a/\tan B)$  values. The final output file called **atn** is an *integer\*2* file containing the  $\ln(a/\tan B)$  values multiplied by 100 (to get two digits to the right of the decimal place and keep an integer format). Missing values are denoted by large negative numbers. Missing values of  $\ln(a/\tan B)$  occur where  $\tan B$  is not calculated at the edge of the map.

```
>atanb
GIVE THE COUNT,SLOPE
AND ATANB FILE NAMES:
num
slo
atn
GIVE VALUES FOR NL AND
NS:
10
10
GIVE THE GRID SPACING:
30
```

6. Use the program **atnmom** to compute the mean, variance, and skew of the  $\ln(a/\tan B)$  distribution. Values for the mean, variance, and skew, the number of  $\ln(a/\tan B)$  values in the file (nobs), and the minimum and maximum values are written to the console. The moments of the spatial distribution can be used to compute a frequency distribution. (See the following section.)

```
>atnmom
Give the binary data input file
name:
```

```
atn
Give values for nl and ns:
10
10
Mean= 6.164689
Var= 1.839231
Skew= 2.490356
Nobs= 64
Min= 4.500000
Max= 9.780000
```

### Frequency Distribution of $\ln(a/\tan B)$

TOPMODEL can be used with the  $\ln(a/\tan B)$  frequency distribution instead of the spatial distribution. When the frequency distribution is used, the moments of the distribution are specified to calculate the three parameters of a shifted gamma distribution (Benjamin and Cornell, 1970), which then is used to generate the relative frequency distribution (fig. 9). The distribution function is given by:

$$p(x) = \frac{v^\eta x^{\eta-1} e^{-vx}}{\Gamma(\eta)}, \quad (46)$$

where  $p(\cdot)$  is probability,  $x$  is the scaled value of  $\ln(a/\tan B)$ ,  $\Gamma(\cdot)$  is the gamma function, and  $v$  and  $\eta$  are parameters. The  $\ln(a/\tan B)$  value is scaled as:

$$x = x_{orig} - \delta \quad (47)$$

if the distribution is positively skewed, and as:

$$x = \delta - x_{orig} \quad (48)$$

if the distribution is negatively skewed.  $\delta$  is a shift parameter, and  $x_{orig}$  is the unscaled value of  $\ln(a/\tan B)$ . The parameters  $\eta$  and  $v$  are estimated from the second ( $M_2$ ) and third ( $M_3$ ) moments about the mean of the distribution as:

$$\eta = \frac{4M_2^3}{M_3^2}, \quad (49)$$

and

$$v = \sqrt{\frac{\eta}{M_2}}. \quad (50)$$

The scaling parameter is estimated as:

$$\delta = M_1 - \frac{\eta}{v} \quad (51)$$

if the distribution is positively skewed, and as:

$$\delta = M_1 + \frac{\eta}{v} \quad (52)$$

if the distribution is negatively skewed.  $M_1$  is the mean of the spatial distribution.

### Spatial and Frequency Distributions of $\ln[a/(T_0 \tan B)]$

$T_0$  is estimated from soil hydraulic data using equation 41 to compute the spatial distribution of  $\ln[a/(T_0 \tan B)]$ . Values of  $T_0$  are determined on the same grid scale as the elevation map used to compute  $\ln(a/\tan B)$  and combined with the values of  $a$  and  $\tan B$  to derive the spatial distribution of  $\ln[a/(T_0 \tan B)]$ . The frequency distribution of  $\ln[a/(T_0 \tan B)]$  is calculated in the same way as for the  $\ln(a/\tan B)$  distribution; that is, by fitting a gamma probability density function to the mean, variance, and skew.

### Channel-Routing Parameters

In the channel-routing algorithm (equation 38), estimates of channel velocity and longest stream length are required. Channel velocity can be set to an assumed value based on empirical relations (for example, see Dunne and Leopold, 1978). The length of the longest stream channel ( $d_{max}$  [L]) can be derived from topographic maps or estimated crudely from watershed area ( $A$  [ $L^2$ ]) as:

$$d_{max} = 2 \sqrt{\frac{A}{\pi}} \quad (53)$$

This simplified relation assumes the watershed is a circle, and the longest stream channel is equal to its diameter.

### Calibration of Model Parameters

Model calibration to a specific watershed is accomplished by setting fixed model parameters, specifying climatic-forcing functions (precipitation and temperature), and determining the values for the calibrated parameters

that give the best agreement between observed and predicted flow.

A time series of precipitation and temperature is necessary to drive the model to generate flow predictions to be compared with the flow observations. Even though TOPMODEL can be run at any time step, the temporal resolution of the data needs to match the time scale of the dynamics in the theoretical framework of the model. This time scale is thought to be on the order of hours. Often, however, hourly precipitation and temperature data are not available. When daily data are used, the model can be run at shorter time steps, and the precipitation input can be distributed over discrete time intervals within a day if information on within-day distributions is available.

The time step of the flow data used for calibration does not necessarily have to match the time step of the precipitation and temperature data. The model can be run at daily time steps, and if only monthly flow data are available for calibration, the daily predicted flows can be aggregated up to a month and compared to the observed monthly flow. Monthly flow data for calibration do not constrain the dynamics of the model to a realistic time frame and, therefore, provide a less realistic model calibration than calibration to daily flows.

TOPMODEL is calibrated to a watershed by determining the combination of adjustable parameter values that minimizes an objective function. The objective function is a mathematical expression that "compares" the observed and predicted streamflows and returns a low value when there is good agreement between the model output and observed data. A calibration is achieved by exploring the response surface of the model, which in a  $p$ -parameter case is defined by calculating values of the objective function and plotting it as the  $p+1$  dimension. The goal in a model calibration, then, is to find the lowest point on the response surface, referred to as the optimum.

A typical expression used as an objective function is the sum of the squared errors (SSE) between the observed and predicted flows, given by:

$$SSE = \sum_{i=1}^n (qobs_i - qpred_i)^2, \quad (54)$$

where  $qobs_i$  is the observed flow at time step  $i$ ,  $qpred_i$  is the predicted flow at time step  $i$ , and  $n$  is the number of time steps. The time series of  $qpred_i$  is generated by specifying the model parameters (adjustable and fixed) and the input series of precipitation and temperature and then running the model.

To locate the optimum parameter set, the model must be run repeatedly, and the  $SSE$  calculated for each model simulation. A computationally efficient method to locate the optimum is to use a directed search of the response surface. The search is "directed" by recording the  $SSE$  for a number of model simulations with different parameter sets and using an algorithm to choose the next parameter set, such that it results in a decrease in the  $SSE$ . A frequently encountered problem in optimization is the termination of the search at a local minimum, that is not the global minimum. This problem often is overcome by repeating the optimization multiple times with different randomly determined starting points.

One commonly used directed-search optimization method is the Rosenbrock algorithm (Rosenbrock, 1960; Rosenbrock and Storey, 1966). In this algorithm, an initial vector of parameter values  $\mathbf{x}^1$  is selected randomly, and the objective function is evaluated [denoted  $F(\mathbf{x}^1)$ ]. The purpose of the optimizing routine is to choose a change in  $\mathbf{x}$  (denoted as  $\mathbf{E}^1$ ) such that  $F(\mathbf{x}^2)$  defined as:

$$F(\mathbf{x}^2) = F(\mathbf{x}^1 + \mathbf{E}^1) \quad (55)$$

is less than  $F(\mathbf{x}^1)$ . The objective is to choose both the direction and step length of  $\mathbf{E}^1$ . If the orthogonal directional vectors of  $\mathbf{E}^1$  are  $[v_1 \dots v_p]$  (for the  $p$  parameters) and the step lengths are  $[e_1 \dots e_p]$ , then  $\mathbf{E}^1$  is defined by  $[e_1 v_1 \dots e_p v_p]$ . After each evaluation of  $F$ ,  $F(\mathbf{x} + \mathbf{E})$  is compared to the lowest value of  $F$  obtained so far ( $F_0$ ). If  $F(\mathbf{x} + \mathbf{E})$  is less than or equal to  $F_0$ , then the parameter set is moved from  $\mathbf{x}$  to  $\mathbf{x} + \mathbf{E}$ , and  $F_0$  is replaced by  $F(\mathbf{x} + \mathbf{E})$ . If  $F(\mathbf{x} + \mathbf{E})$  is greater than  $F_0$ , then the parameter set and  $F_0$  are left unmodified. After each evaluation of  $F$ ,  $\mathbf{E}$  is also modified. If the new  $F$  is less than the old  $F$ , then  $\mathbf{E}$  is increased, and if the new  $F$  is greater than the old  $F$ , then  $\mathbf{E}$

is decreased. Evaluations of  $F$  are continued until an increase in the  $SSE$  has occurred in every direction  $[v_1 \dots v_p]$ . Then,  $[v_1 \dots v_p]$  is replaced by a new set of orthogonal vectors,  $[v_1 \dots v_p]^{new}$  as follows. First, the algebraic sums  $[d_1 \dots d_p]$  of all the successful steps  $[e_1 \dots e_p]$  in the directions  $[v_1 \dots v_p]$  are computed. The vector sums  $[A_1 \dots A_p]$  then are calculated as:

$$A_1 = d_1 v_1 + d_2 v_2 + \dots + d_p v_p, \quad (56)$$

$$A_2 = d_2 v_2 + \dots + d_p v_p, \quad (57)$$

$$A_p = d_p v_p. \quad (58)$$

Finally, new directions  $[v_1 \dots v_p]^{new}$  are calculated as:

$$B_1 = A_1, \quad (59)$$

$$v_1^{new} = \frac{B_1}{|B_1|}, \quad (60)$$

$$B_2 = A_2 - A_1 v_1^{new} v_1^{new}, \quad (61)$$

$$v_2^{new} = \frac{B_2}{|B_2|}, \quad (62)$$

$$B_p = A_p - \sum_{i=1}^{p-1} (A_p v_i^{new} v_i^{new}), \text{ and } \quad (63)$$

$$v_p^{new} = \frac{B_p}{|B_p|}, \quad (64)$$

where  $| \cdot |$  is the absolute value. After the new directions  $[v_1 \dots v_p]^{new}$  are determined, the parameter space can be searched along these directions for a lower  $SSE$ . The optimization continues until there is no further improvement in the objective function or until the magnitudes of the changes in the parameter values are less than a specified nominal level.

## USING THE TOPMODEL FORTRAN PROGRAM

The Fortran code for TOPMODEL is structured in a modular format. A flow chart showing the relations among the main components and their functions is illustrated in figure 15. The



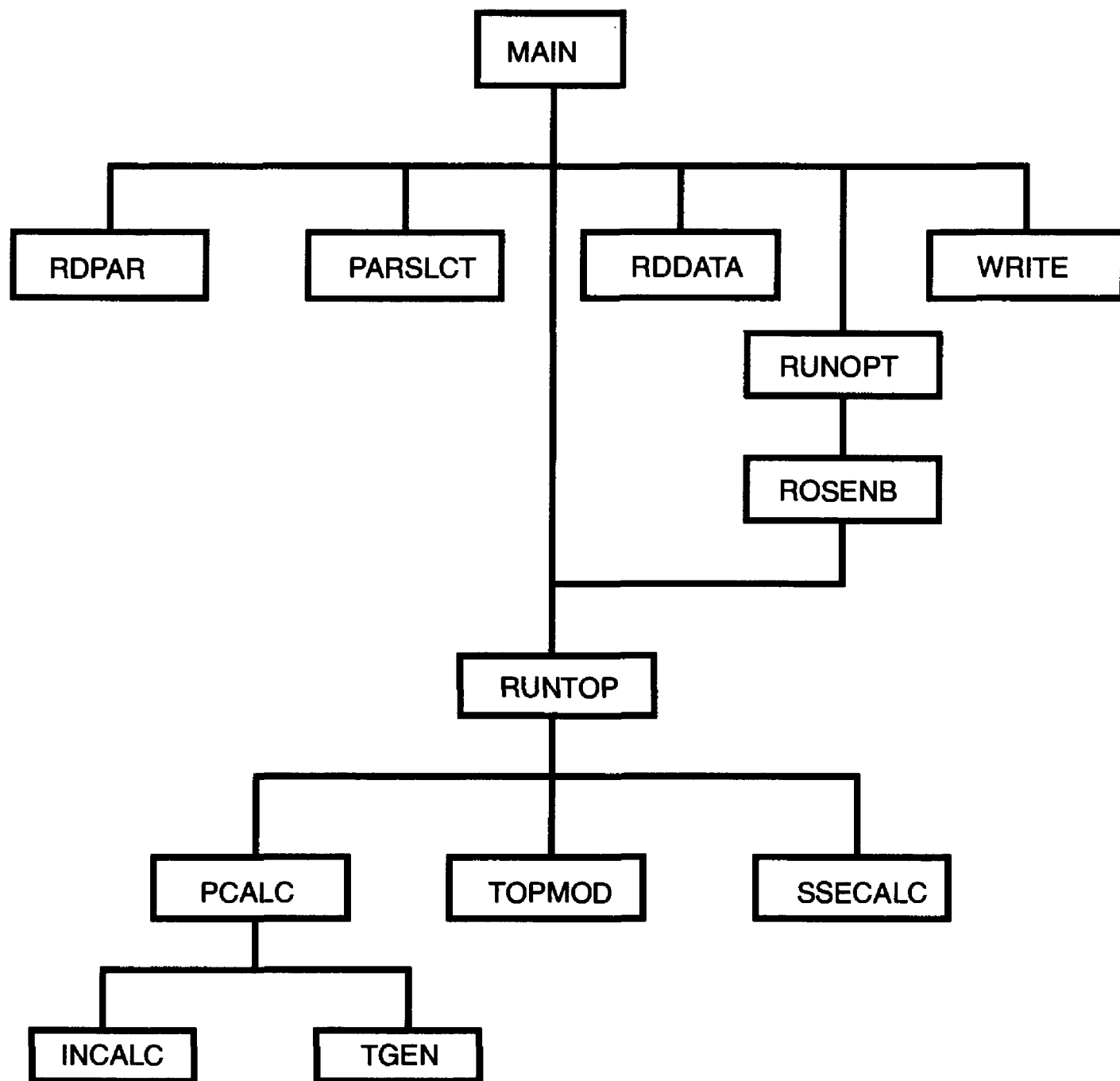


**Figure 15.** Relations among major TOPMODEL components. MAIN prompts user for optimization information; RDPAR reads in parameter-information file and prompts user for the length of a time step; PARSLCT changes parameter values and selects parameters for optimization; RDDATA reads in input data, computes initial time series of snowpack accumulation, snowmelt, and potential evapotranspiration; RUNTOP initializes model states; PCALC computes internal parameters values; TGEN computes frequency distribution of  $\ln(a/\tan B)$  from statistical moments of the  $\ln(a/\tan B)$  distribution; INCALC computes time series of snowpack accumulation, snowmelt, and potential evapotranspiration when parameters affecting these states are optimized; TOPMOD computes evapotranspiration, soil-moisture balance, changes in the saturation deficit, overland flow, subsurface flow, and channel routing; RUNOPT initializes Rosenbrock optimization; ROSENB performs Rosenbrock optimization; SSECALC computes goodness-of-fit statistics that are optimized; and WRITE writes output variables to file named top.out.

particular code described here runs the model in the frequency domain of  $\ln(a/\tan B)$ .

The parameter file has five columns: parameter name, default value, minimum value, maximum value, and flag value (table 3). The minimum, maximum, and flag values are

used in parameter calibration. The minimum and maximum set the outer bounds on the range that can be used in the calibration. The flag value determines whether the parameter space is searched linearly (flag = 0.) or logarithmically (flag = 1.). The code is written so that a parameter value of -99. either sets the default

**Table 3. Contents of parameter file for TOPMODEL**

[Default, default value; Min, minimum value; Max, maximum value; Flag, optimization flag value; SZM, scaling parameter based on soil properties; CONMEAN, saturated hydraulic conductivity of the C horizon of the soil; PMAC, fraction of precipitation bypassing soil zone; ZTOT, total soil depth; ZAB, depth of AB horizon; THFC, field capacity of soil; TOPMEAN, mean of  $\ln(a/\tan B)$  distribution; TOPVAR, variance of  $\ln(a/\tan B)$  distribution; TOPSKEW, skew of  $\ln(a/\tan B)$  distribution; XLAT, latitude; ATOT, total watershed area; TCUT, temperature cutoff for snowpack accumulation and snowmelt; PIMP, impervious area of watershed]

Parameter name	Default	Min	Max	Flag
SZM	10.	5.	100.	0.
CONMEAN	150.	50.	2000.	0.
PMAC	0.2	0.	0.5	0.
ZTOT	1.	1.	5.	0.
ZAB	0.5	0.3	0.6	0.
THFC	0.2	0.05	0.3	0.
TOPMEAN	6.94	6.	9.	0.
TOPVAR	2.05	1.	4.	0.
TOPSKEW	3.73	2.	5.	0.
XLAT	40.5	35.	40.	0.
ATOT	3.07	0.8	10.	0.
TCUT	-99.	20.	40.	0.
PIMP	0.3	0.	0.5	0.

value to an internally declared value or turns off a component of the model. For example, the value of TCUT in table 3 is set to -99., thereby turning off the snow-accumulation and melt component of the model. This module was not used in this example because previous knowledge of the basin indicated that snow accumulation and melt played no role in the hydrologic response of the watershed. The snow module was not used because including it would have the potential to confound the results.

The parameter and variable names in the Fortran code are not all the same as those used in this report. A list of the corresponding parameter and variable names and definitions are given in tables 4 and 5. Some of the parameter names in table 4 do not appear in table 3. The values of these parameters are set internally in the code.

The input meteorologic and hydrologic data file has six columns: year, month, day, flow [*millimeters per day*], precipitation [*millimeters per day*], and temperature [*degrees Celsius*]. An example file is given in table 6.

An example session of using TOPMODEL in UNIX is given below. Keyboard input supplied by the user is written in bold. Console output

from the program is printed in italics. Commentary is written in normal text.

The model is run by typing **topmodel**, which is the name of the compiled and linked run file. The parameter file and input data file must be in the directory where the model is being run. In this example, the parameter file is called **proy**, and the input data file is called **droy**. The contents of **proy** and **droy** are shown in tables 3 and 6, respectively.

**>topmodel**

*GIVE THE PARAMETER FILE NAME:*

**proy**

The time-step length given below must match that of the input data. For example, if the time step of the input data is 1 day, then 1,440 minutes is entered here.

*GIVE THE TIME STEP LENGTH IN MINUTES:*

**1440**

The default parameter values are used in the simulation unless they are changed below. The default values will be used as the starting point in an optimization if that option is selected. A default value of -99.0 for TCUT is a flag to turn off the snowmelt and accumulation algorithm of the model.

**Table 4.** Corresponding parameter names in TOPMODEL Fortran code and in this report

Fortran code	This report	Definition	Units
SZM	$m$	Scaling parameter based on soil properties	millimeters
CONMEAN	$K$	Saturated hydraulic conductivity of the C horizon of the soil	millimeters per day
PMAC	$p_{macro}$	Fraction of precipitation bypassing soil zone	fraction
ZTOT	$z_{tot}$	Total soil depth (AB+C)	meters
ZAB	$z_{ab}$	Depth of AB horizon	meters
THFC	$\theta_{fc}$	Field capacity of soil	fraction
TOPMEAN, TL	$M_1 (\lambda)$	Mean of $\ln(a/\tan B)$ distribution	$\ln(\text{meters})$
TOPVAR	$M_2$	Variance of $\ln(a/\tan B)$ distribution	$\ln(\text{meters})^2$
TOPSKEW	$M_3$	Skew of $\ln(a/\tan B)$ distribution	$\ln(\text{meters})^3$
XLAT	$latitude$	Latitude	degrees
ATOT	$A$	Total watershed area	square kilometers
TCUT	$T_{cut}$	Temperature cutoff for snowpack accumulation and snowmelt	degrees Fahrenheit
PIMP	$p_{imp}$	Impervious area of watershed	fraction
SNOPROP	$p_{snow}$	Snowmelt parameter	inches per degree Fahrenheit
RAINPRO	$p_{rain}$	Rain-induced snowmelt parameter	1/degrees Fahrenheit
SRMAX	$D_{root}$	Maximum root-zone storage	millimeters of water
ZROOT	$z_{root}$	Root-zone depth	meters
DMAX	$d_{max}$	Maximum channel length	kilometers
SUBV	$v$	Channel velocity	kilometers per day
TOPETA	$v$	Gamma distribution parameter	--
TOPLAM	$\eta$	Gamma distribution parameter	--
GAMLN	$\Gamma$	Gamma function	--
TOPSCAL	$\delta$	Gamma distribution parameter	--
SZQ	$q_{submax}$	Maximum subsurface flow rate	millimeters per day
TRANS	$T_0$	Maximum saturated transmissivity	square millimeters per day
ST	$\ln(a/\tan B)$	$\ln(a/\tan B)$ value	$\ln(\text{meters})$

**THE DEFAULT VALUES ARE:**

1 SZM	10.0	2 CONMEAN	150.
3 PMAC	0.200	4 ZTOT	1.0
5 ZAB	0.500	6 THFC	0.200
7 TOPMEAN	6.94	8 TOPVAR	2.05
9 TOPSKEW	3.73	10 XLAT	40.5
11 ATOT	3.07	12 TCUT	-99.0
13 PIMP	0.300		

The default value can be changed by entering its code. For example, to change the value of SZM, enter 1 here. The user then is prompted for the new value. When no more values are to be changed, then the code 0 (zero) is entered.

**GIVE THE CODE OF THE DEFAULT VALUE TO CHANGE:**

**(TYPE 0 WHEN DONE)**

0

These values set the minimum values of the ranges used in the optimization.

**THE MINIMUM VALUES ARE:**

1 SZM	5.00	2 CONMEAN	50.0
3 PMAC	0.000E+00	4 ZTOT	1.00
5 ZAB	0.300	6 THFC	0.500E-01
7 TOPMEAN	6.00	8 TOPVAR	1.00
9 TOPSKEW	2.00	10 XLAT	35.0
11 ATOT	0.800	12 TCUT	20.0
13 PIMP	0.000E+00		

**GIVE THE CODE OF THE MINIMUM VALUE TO CHANGE:**

**(TYPE 0 WHEN DONE)**

0

**Table 5. Corresponding variable names in TOPMODEL Fortran code and in this report**

Fortran code	This report	Definition	Units
QPREL	$q_{total}$	Total predicted flow	millimeters per day
QOF	$q_{overland}$	Predicted overland flow	millimeters per day
QB	$q_{subsurface}$	Predicted subsurface flow	millimeters per day
AC	$a_{sat}$	Saturated land-surface area in watershed	fraction
PP, P, PPT	$i$	Precipitation	millimeters per day
S	$\bar{S}$	Watershed average saturation deficit	millimeters of water
SD	$S_x$	Saturation deficit at location x	millimeters of water
UZ	$q_{drain}$	Vertical drainage flux	millimeters per day
SUZ	$w_{drain}$	Soil water available for drainage	millimeters of water
PPEX	$ex_{et}$	Precipitation in excess of evapotranspiration and field-capacity storage	millimeters of water
XMELT	$d_{melt}, d_{rain}$	Snowmelt	millimeters of water
DENS	$\rho$	Mass density of water in air	grams per cubic meter multiplied by 0.01
DAYLEN	$D$	Maximum possible clear-sky duration of sunshine	hours/12
QQ	$q_{portion}$	Flow delivered to stream channel	millimeters per day
NTW	$t_{steps}$	Channel travel time	days
PET	$PET$	Potential evapotranspiration	millimeters
TEMP, T	$Temp$	Temperature	degrees Celsius
QOBS, Q	$q_{obs}$	Observed flow	millimeters per day

These values set the maximum values of the ranges used in the optimization.

**THE MAXIMUM VALUES ARE:**

1 SZM 100. 2 CONMEAN 0.200E+04  
3 PMAC 0.500 4 ZTOT 5.00  
5 ZAB 0.600 6 THFC 0.300  
7 TOPMEAN 9.00 8 TOPVAR 4.00  
9 TOPSKEW 5.00 10 XLAT 40.0  
11 ATOT 10.0 12 TCUT 40.0  
13 PIMP 0.500

**GIVE THE CODE OF THE MAXIMUM VALUE TO CHANGE:**

(TYPE 0 WHEN DONE)

0

The parameters corresponding to the codes listed here will be optimized.

**GIVE THE CODES OF THE PARAMS TO OPTIMIZE:**

(TYPE 0 WHEN DONE)

1

3

0

**GIVE THE INPUT DATA FILE NAME:**

**droy**

The model should be "warmed-up" for a number of time steps before the predicted flow is compared to the observed flow to compute the objective function (OBJ FN). The warm-up is necessary because a number of model states are initialized arbitrarily at the beginning of the simulation, and the warm-up period dampens out possible errors from the initial conditions.

**GIVE THE FIRST STEP FOR OBJ FN EVALUATION:**

**366**

The objective function can be evaluated in logarithmic or linear space. Evaluation in logarithmic space tends to give equal weight to low, medium, and high flows. Evaluation in linear space gives greater weight to high flows.

**TYPE 1 FOR OBJ FN IN LOG SPACE, 0 FOR LINEAR:**

0

The efficiency using the default params is: 0.55

**Table 6. Contents of input data file for TOPMODEL**

[Flow, streamflow in millimeters per day; Precip, precipitation in millimeters per day;  
Temp, temperature in degrees Celsius]

Year	Month	Day	Flow	Precip	Temp
1980	1	22	1.18	2.5	-1.9
1980	1	23	1.02	0.0	-0.3
1980	1	24	0.66	0.0	-1.1
1980	1	25	0.50	0.0	-6.1
1980	1	26	0.46	0.0	-4.7
1980	1	27	0.40	0.0	-4.4
1980	1	28	0.39	0.0	-3.3
1980	1	29	0.33	0.0	-3.1
1980	1	30	0.28	0.0	-4.2
1980	1	31	0.24	0.0	-5.6
1980	2	1	0.19	0.0	-7.2
1980	2	2	0.20	0.0	-9.4
1980	2	3	0.21	0.0	-9.4
1980	2	4	0.24	0.0	-7.2
1980	2	5	0.27	0.0	-6.4
1980	2	6	0.28	0.0	-5.6
1980	2	7	0.24	0.0	-6.7

TYPE 1 FOR OPTIMIZATION, 0 IF  
NOT:  
1

9.108 0.200 0.565

...  
5.046 0.002 0.705

The TOLERANCE is the minimum proportional change in a parameter that is considered significant. The maximum number of iterations (MAX ITERATIONS) is the maximum number of times that the parameter space is explored by the optimizing algorithm.

5.001 0.015 0.704

5.334 0.000 0.706

5.972 0.006 0.706

5.466 0.000 0.707

5.466 0.000 0.707

GIVE VALUE FOR TOLERANCE AND  
MAX ITERATIONS:  
(.01 AND 2 ARE RECOMMENDED  
VALUES)

.01

2

The calibration info is being written to a  
file called top.cal

SZM	PMAC	EFFI
10.000	0.200	0.550
10.198	0.200	0.546
9.805	0.200	0.553
9.520	0.200	0.558

Entering 0 terminates the simulation, and  
the output data are written to the file top.out.  
Entering 1 loops the program back to the  
beginning.

TYPE 1 TO TRY AGAIN, 0 IF NOT:  
0

The contents of an example output file are  
given in table 7. The first line of the output file  
contains the number of variables in the file, and  
the second line gives variable names. The  
remaining lines give output values for each time  
step. The four output variables in table 7 are  
time (measured in time steps since the  
beginning of the simulation), precipitation

**Table 7. Contents of output file from TOPMODEL**

[TIME, number of time steps since the beginning of the simulation; PPT-PET, precipitation minus potential evapotranspiration in millimeters per day; QOBSERVED, observed streamflow in millimeters per day; QPREDICT, predicted streamflow in millimeters per day]

TIME	PPT-PET	QOBSERVED	QPREDICT
1.000	2.108	1.180	1.225
2.000	-0.436	1.020	1.175
3.000	-0.418	0.660	0.948
4.000	-0.308	0.500	0.797
5.000	-0.338	0.460	0.689
6.000	-0.347	0.400	0.607
7.000	-0.374	0.390	0.543
8.000	-0.381	0.330	0.492
9.000	-0.358	0.280	0.450
10.000	-0.331	0.240	0.414
11.000	-0.302	0.190	0.384
12.000	-0.265	0.200	0.358
13.000	-0.267	0.210	0.335
14.000	-0.308	0.240	0.315
15.000	-0.326	0.270	0.298
16.000	-0.345	0.280	0.282
17.000	-0.325	0.240	0.268
18.000	-0.433	0.250	0.255
19.000	-0.444	0.310	0.243
20.000	-0.403	0.320	0.233

minus potential evapotranspiration [millimeters per day], observed flow [millimeters per day], and predicted flow [millimeters per day].

*The output data are being written to a file called top.out*

## **POTENTIAL FUTURE DIRECTIONS FOR TOPMODEL**

Future directions in the evolution of TOPMODEL will be determined in part by the research activities of the investigators actively using the model. Ongoing research areas involving TOPMODEL are listed below:

- (1) Effects of watershed hydrologic processes on forest succession. TOPMODEL has been coupled to a forest ecosystem model (L.E. Band, University of Toronto, written commun., 1992).

- (2) Effects of parameter uncertainty on model predictions. A calibration method called the Generalized Likelihood Uncertainty Estimation (GLUE) technique has been incorporated in a version of TOPMODEL (K.J. Beven, University of Lancaster, written commun., 1992).

- (3) Visualization of predictions from spatially distributed models. TOPMODEL code has been incorporated into software that facilitates visualization of model predictions as they change over time and space (S. Timmons, Oak Ridge National Laboratory, written commun., 1992).

- (4) Effects of spatial data resolution on hydrologic processes. Several research groups are evaluating the effects of digital elevation-data resolution on computation of the  $\ln(a/\tan B)$  distribution and subse-

quent effects on TOPMODEL predictions (L.E. Band, University of Toronto, written commun., 1992; Wolock and Price, 1989).

- (5) Development of user-friendly watershed-modeling tools. The variable-source-area concept, as it is represented in TOPMODEL, has been developed into a module in the Modular Hydrologic Modeling System (Leavesley and others, 1992), which includes simulation modules of varying complexity of many hydrologic processes in watershed hydrology. Also, efforts are underway to include modules simulating important processes affecting water quality, such as the fate and transport of nutrients and pesticides, so that elements of TOPMODEL can be combined with water-quality modules to address fate and transport problems at the watershed scale.

## REFERENCES

- Anderson, M.G., and Burt, T.P., 1978, The role of topography in controlling throughflow generation: *Earth Surface Processes*, v. 3, p. 331-344.
- Anderson, M.G., and Kneale, P.E., 1980, Topography and hillslope soil water relationships in a catchment of low relief: *Journal of Hydrology*, v. 47, p. 115-128.
- Band, L.E., Petersen, D.L., Running, S.W., Coughlan, J.C., Lammers, R.B., Dungan, J., and Nemani, R., 1991, Forest ecosystem processes at the watershed scale--Basis for distributed simulation: *Ecological Modeling*, v. 56, p. 151-176.
- Bathurst, J.C., 1986, Sensitivity analysis of the Systeme Hydrologique European for an upland catchment: *Journal of Hydrology*, v. 87, p. 103-123.
- Benjamin, J.R., and Cornell, C.A., 1970, Probability, statistics and decision for civil engineers: New York, McGraw Hill, 684 p.
- Bernier, P.Y., 1985, Variable source areas and storm-flow generation--An update of the concept and a simulation effort: *Journal of Hydrology*, v. 79, p. 195-213.
- Betson, R.P., 1964, What is watershed runoff?: *Journal of Geophysical Research*, v. 69, p. 1541-1552.
- Beven, K.J., 1978, The hydrological response of headwater and sideslope areas: *Hydrological Sciences Bulletin*, v. 23, p. 419-437.
- \_\_\_\_\_, 1984, Infiltration into a class of vertically nonuniform soils: *Hydrological Sciences Journal*, v. 29, p. 425-434.
- \_\_\_\_\_, 1986a, Runoff production and flood frequency in catchments of order n--An alternative approach, in Gupta, V.K., Rodriguez-Iturbe, I., and Wood, E.F., eds., *Scale problems in hydrology*: Dordrecht, D. Reidel Publ. Co., p. 107-131.
- \_\_\_\_\_, 1986b, Hillslope runoff processes and flood frequency characteristics, in Abrahams, A.D., ed., *Hillslope processes*: London, Allen and Unwin, p. 187-202.
- \_\_\_\_\_, 1987, Towards the use of catchment geomorphology in flood frequency predictions: *Earth Surface Processes and Landforms*, v. 12, p. 69-82.
- Beven, K.J., and Germann, P., 1982, Macropores and water flow in soils: *Water Resources Research*, v. 18, p. 1311-1325.
- Beven, K.J., and Kirkby, M.J., 1979, A physically based, variable contributing area model of basin hydrology: *Hydrological Sciences Bulletin*, v. 24, p. 43-69.
- Beven, K.J., Kirkby, M.J., Schofield, N., and Tagg, A.F., 1984, Testing a physically-based flood forecasting model (TOPMODEL) for three U.K. catchments: *Journal of Hydrology*, v. 69, p. 119-143.
- Beven, K.J., and Wood, E.F., 1983, Catchment geomorphology and the dynamics of runoff contributing areas: *Journal of Hydrology*, v. 65, p. 139-158.
- Beven, K.J., Wood, E.F., and Sivapalan, M., 1988, On hydrological heterogeneity--Catchment morphology and catchment response: *Journal of Hydrology*, v. 100, p. 353-375.



- Binley, A., Elgy, J., and Beven, K., 1989, A physically based model of heterogeneous hillslopes, 1. Runoff production: *Water Resources Research*, v. 25, p. 1219-1226.
- Burt, T.P., and Butcher, D.P., 1985, Topographic controls of soil moisture distributions: *Journal of Soil Science*, v. 36, p. 469-486.
- Chow, V.T., 1964, *Handbook of applied hydrology*: New York, McGraw Hill, 1418 p.
- Cosby, B.J., Hornberger, G.M., Ginn, T.R., and Clapp, R.B., 1984, A statistical exploration of the relationships of soil moisture characteristics to the physical properties of soils: *Water Resources Research*, v. 20, p. 682-690.
- Dunne, T., and Black, R.D., 1970, Partial area contributions to storm runoff in a small New England watershed: *Water Resources Research*, v. 6, p. 1296-1311.
- Dunne, T., and Leopold, L.B., 1978, *Water in environmental planning*: New York, W.H. Freeman and Company, 818 p.
- Dunne, T., Moore, T.R., and Taylor, C.H., 1975, Recognition and prediction of runoff-producing zones in humid regions: *Hydrological Sciences Bulletin*, v. 20, p. 305-327.
- Elassal, A.A., and Caruso, V.M., 1983, Digital elevation models: U.S. Geological Survey Circular 895-B, 40 p.
- Elsenbeer, H., Cassel, K., and Castro, J., 1992, Spatial analysis of soil hydraulic conductivity in a tropical rain forest catchment: *Water Resources Research*, v. 28, p. 3201-3214.
- Famiglietti, J.S., 1992, *Aggregation and scaling of spatially-variable hydrological processes--Local, catchment-scale and macro-scale models of water and energy balance*: Princeton, Princeton University, October 1992, Ph.D. dissertation, 207 p.
- Famiglietti, J.S., and Wood, E.F., 1991, Evapotranspiration and runoff from large land areas--Land surface hydrology for atmospheric general circulation models: *Surveys of Geophysics*, v. 12, p. 179-204.
- Freeze, R.A., 1980, A stochastic-conceptual analysis of rainfall-runoff processes on a hillslope: *Water Resources Research*, v. 16, p. 391-408.
- Grayson, R.B., Moore, I.D., and McMahon, T.A., 1992, Physically based hydrologic modeling, 1. A terrain-based model for investigative purposes: *Water Resources Research*, v. 28, p. 2639-2658.
- Hamon, W.R., 1961, Estimating potential evapotranspiration: *Journal of the Hydraulics Division, Proceedings of the American Society of Civil Engineers*, v. 87, p. 107-120.
- Hewlett, J.D., and Hibbert, A.R., 1967, Factors affecting the response of small watersheds to precipitation in humid areas, in Sopper, W.E., and Lull, H.W., eds., *Forest hydrology*: New York, Pergamon Press.
- Hornberger, G.M., Beven, K.J., Cosby, B.J., and Sappington, D.E., 1985, Shenandoah watershed study--Calibration of a topography-based, variable contributing area hydrological model to a small forested catchment: *Water Resources Research*, v. 21, p. 1841-1850.
- Horton, R.E., 1933, The role of infiltration in the hydrologic cycle: *EOS, Transactions, American Geophysical Union*, v. 14, p. 446-460.
- Hursh, C.R., 1936, Storm water and absorption: *Transactions of the American Geophysical Union*, part II, p. 301-302.
- Ijjasz-Vasquez, E.J., Bras, R.L., and Moglen, G.E., 1992, Sensitivity of a basin evolution model to the nature of runoff production and to initial conditions: *Water Resources Research*, v. 28, p. 2733-2741.
- Jenson, S.K., and Domingue, J.O., 1988, Extracting topographic structure from digital elevation data for geographic information system analysis: *Photogrammetric Engineering and Remote Sensing*, v. 54, p. 1593-1600.

- Keith, F., and Kreider, J.F., 1978, Principles of solar engineering: Washington, D.C., Hemisphere Publ. Corp.
- Kennedy, V.C., Kendall, C., Zellweger, G.W., Wyerman, T.A., and Avanzino, R.J., 1986, Determination of the components of storm-flow using water chemistry and environmental isotopes, Mattole River Basin, California: *Journal of Hydrology*, v. 84, p. 107-140.
- Kirkby, M., 1986, A runoff simulation model based on hillslope topography, in Gupta, V.K., Rodriguez-Iturbe, I., and Wood, E.F., eds., *Scale problems in hydrology*: Dordrecht, D. Reidel Publ. Co., p. 39-56.
- Kirkby, M.J., and Chorley, R.J., 1967, Through-flow, overland flow and erosion: *Bulletin of the International Association of Scientific Hydrology*, v. 12, p. 5-21.
- Leavesley, G.H., Restrepo, P., Stannard, L.G., and Dixon, M., 1992, The Modular Hydrologic Modeling System--MHMS, in 28th Annual Conference and Symposium, Managing Water Resources During Global Change, Reno, Nev., November 1-5, 1992, Proceedings: American Water Resources Association, p. 263-264.
- Lee, M.T., and Delleur, J.W., 1976, A variable source area model of the rainfall runoff process based on the watershed stream network: *Water Resources Research*, v. 12, p. 1029-1036.
- Moore, I.D., and Grayson, R.B., 1991, Terrain-based catchment partitioning and runoff prediction using vector elevation data: *Water Resources Research*, v. 27, p. 1177-1191.
- Moore, I.D., Mackay, S.M., Wallbrink, G.J., Burch, G.J., and O'Loughlin, E.M., 1986, Hydrologic characteristics and modelling of a small forested catchment in south-eastern New South Wales--Prelogging condition: *Journal of Hydrology*, v. 83, p. 307-335.
- Mosley, M.P., 1979, Streamflow generation in a forested watershed, New Zealand: *Water Resources Research*, v. 15, p. 795-806.
- O' Loughlin, E.M., 1981, Saturation regions in catchments and their relations to soil and topographic properties: *Journal of Hydrology*, v. 53, p. 229-246.
- \_\_\_\_\_, 1986, Prediction of surface saturation zones in natural catchments by topographic analysis: *Water Resources Research*, v. 22, p. 794-804.
- Ormsbee, L.E., and Khan, A.Q., 1989, A parametric model for steeply sloping forested watersheds: *Water Resources Research*, v. 25, p. 2053-2065.
- Pearce, A.J., Stewart, M.K., and Sklash, M.G., 1986, Storm runoff generation in humid headwater catchments, 1. Where does the water come from?: *Water Resources Research*, v. 22, p. 1263-1271.
- Prevost, M., Barry, R., Stein, J., and Plamondon, A.P., 1990, Snowmelt runoff modeling in a Balsam Fir forest with a variable source area simulator (VSAS2): *Water Resources Research*, v. 26, p. 1067-1077.
- Rosenbrock, H.H., 1960, An automatic method for finding the greatest or least value of a function: *Computer Journal*, v. 3, p. 175-184.
- Rosenbrock, H.H., and Storey, C., 1966, *Computational techniques for chemical engineers*: Oxford, Pergamon Press, 328 p.
- Sivapalan, M., Beven, K.J., and Wood, E.F., 1987, On hydrologic similarity, 2. A scaled model of storm runoff production: *Water Resources Research*, v. 23, p. 2266-2278.
- Sivapalan, M., Wood, E.F., and Beven, K.J., 1990, On hydrologic similarity, 3. A dimensionless flood frequency model using a generalized geomorphologic unit hydrograph and partial area runoff generation: *Water Resources Research*, v. 26, p. 43-58.

- Sklash, M.G., and Farvolden, R.N., 1979, The role of groundwater in storm runoff: *Journal of Hydrology*, v. 43, p. 45-65.
- Sklash, M.G., Stewart, M.K., and Pearce, A.J., 1986, Storm runoff generation in humid headwater catchments, 2. A case study of hillslope and low-order stream response: *Water Resources Research*, v. 22, p. 1273-1282.
- Smith, R.E., and Hebbert, R.H.B., 1983, Mathematical simulation of interdependent surface and subsurface hydrologic processes: *Water Resources Research*, v. 19, p. 987-1001.
- Stagnitti, F., Parlange, J.Y., Steenhuis, T.S., Parlange, M.B., and Rose, C.W., 1992, A mathematical model of hillslope and watershed discharge: *Water Resources Research*, v. 28, p. 2111-2122.
- Stephenson, G.R., and Freeze, R.A., 1974, Mathematical simulation of subsurface flow contributions to snowmelt runoff, Reynolds Creek watershed, Idaho: *Water Resources Research*, v. 10, p. 284-294.
- U.S. Army Corps of Engineers, 1960, *Manuals--Engineering and design, runoff from snowmelt: EM1110-2-1406*.
- Whipkey, R.Z., 1965, Subsurface stormflow from forested slopes: *Hydrological Sciences Bulletin*, v. 10, p. 74-85.
- Wolock, D.M., 1988, Topographic and soil hydraulic control of flow paths and soil contact time--Effects on surface water acidification: Charlottesville, University of Virginia, May 1988, 188 p.
- Wolock, D.M., and Hornberger, G.M., 1991, Hydrological effects of changes in atmospheric carbon dioxide levels: *Journal of Forecasting*, v. 10, p. 105-116.
- Wolock, D.M., Hornberger, G.M., Beven, K.J., and Campbell, W.G., 1989, The relationship of catchment topography and soil hydraulic characteristics to lake alkalinity in the northeastern United States: *Water Resources Research*, v. 25, p. 829-837.
- Wolock, D.M., Hornberger, G.M., and Musgrove, T.J., 1990, Topographic effects on flow path and surface water chemistry of the Llyn Brianne catchments in Wales: *Journal of Hydrology*, v. 115, p. 243-259.
- Wolock, D.M., and Price, C.V., 1989, Effects of resolution of digital elevation model data on a topographically based hydrologic model: *EOS, Transactions, American Geophysical Union*, v. 70, p. 1091.
- Wood, E.F., Sivapalan, M., and Beven, K.J., 1986, Scale effects in infiltration and runoff production, in *Conjunctive water use, Proceedings of the Budapest Symposium, July 1986: International Association of Hydrological Sciences Publication 156*, p. 375-387.
- \_\_\_\_\_, 1990, Similarity and scale in catchment storm response: *Reviews of Geophysics*, v. 28, p. 1-18.
- Wood, E.F., Sivapalan, M., Beven, K.J., and Band, L.E., 1988, Effects of spatial variability and scale with implications to hydrologic modeling: *Journal of Hydrology*, v. 102, p. 29-47.